Effects of translational, rotational, and vibrational energy on the dynamics of the D+H2 exchange reaction. A classical trajectory study

F. J. Aoiz, V. J. Herrero, and V. Sáez Rábanos

Citation: The Journal of Chemical Physics **94**, 7991 (1991); doi: 10.1063/1.460133
View online: http://dx.doi.org/10.1063/1.460133
View Table of Contents: http://scitation.aip.org/content/aip/journal/jcp/94/12?ver=pdfcov
Published by the AIP Publishing

Articles you may be interested in

Effects of rotational, vibrational, and translational energy on the rate constants for the isotope exchange reactions OH−+D2 and OD−+H2
J. Chem. Phys. **100**, 2748 (1994); 10.1063/1.466469

Reaction dynamics of D+H2→DH+H: Effects of potential energy surface topography and usefulness of the constant centrifugal potential approximation
J. Chem. Phys. **96**, 339 (1992); 10.1063/1.462522

Comment on: ''H+NO translationtovibration/rotation energy transfer: A classical trajectory study''
J. Chem. Phys. **86**, 3756 (1987); 10.1063/1.451930

Effect of vibration on rotational energy transfer. A quasiclassical trajectory study of He+H2
J. Chem. Phys. **75**, 1829 (1981); 10.1063/1.442206

Quasiclassical trajectory studies of the H+H2 reaction on an accurate potential energy surface. II. Effect of initial vibration and rotation on reactivity
J. Chem. Phys. **74**, 1017 (1981); 10.1063/1.441234

This article is copyrighted as indicated in the article. Reuse of AIP content is subject to the terms at: http://scitation.aip.org/termsconditions. Downloaded to IP: 130.209.6.50 On: Fri, 19 Dec 2014 14:02:13

Effects of translational, rotational, and vibrational energy on the dynamics of the D + H_2 exchange reaction. A classical trajectory study

F. J. Aoiz
Departamento de Química Física, Facultad de Química, Universidad Complutense, 28040 Madrid, Spain

V. J. Herrero
Instituto de Estructura de la Materia (CSIC), Serrano 123, 28006 Madrid, Spain

V. Sáez Rábanos
Departamento de Química General y Bioquímica, ETS Ingenieros de Montes, Universidad Politécnica, 28040 Madrid, Spain

(Received 15 January 1991; accepted 7 March 1991)

Quasiclassical trajectory (QCT) calculations for the D + $H_2(v,j) \rightarrow$ HD + H system have been performed on the Liu, Siegbahn, Truhlar, Horowitz (LSTH) potential energy surface in order to study the combined effects of translation, rotation, and vibration on the reactivity. The range of initial conditions covered has been $E_T = 0.25$–1 eV, $v = 0$, 1, and 2 and $j = 0$–12. Integral cross sections, opacity functions, solid angle differential cross sections, and the energy partitioning among the products' degrees of freedom have been obtained. The minimum in the dependence of the total cross section with rotational excitation observed in previous QCT calculations for $v = 0$ and $v = 1$ at low collision energies is here verified also for $v = 2$. The center-of-mass (c.m.) angular distributions of the scattered HD product are predominantly backward with respect to the direction of the D incoming atom, at low energies, but they broaden markedly and become more forward with increasing total energy. Translational and vibrational excitation in the reactants are largely adiabatic and tend to remain as translation and vibration in the products. Where they can be compared, present results are in good agreement with recent quantum mechanical calculations and with experimental measurements.

I. INTRODUCTION

The role played by translational and by internal energy in chemical change at a molecular level and its relationship to the properties of the potential energy surface (PES) which govern a given reaction has deserved much attention since the early systematizations of Polanyi and co-workers.[1-3] Good reviews covering different aspects of the subject are now available.[4-9] The effects of the specific energy modes on direct reactions of the A + BC type have been studied in detail by means of quasiclassical trajectory (QCT) calculations on both model and real systems with different, mostly semiempirical potential energy surfaces and, when possible, compared to experimental results.[1-3,10,11] Initially, the ease to perform and visualize calculations for collinear collisions attracted much attention to the study of the distinct role of translation and vibration on reaction probability permitting us to gain some insight; in particular, the fact that translational energy (E_T) is more effective in promoting reaction for systems with an early barrier, whereas vibrational energy (E_V) is more efficient for reactions with a late barrier, was clearly established.[12]

More recently, extensive work has also been devoted to the effect of rotational energy (E_R) on reactivity,[6,7,13-22] but in spite of some progress, no simple general assertions can be made about the influence of rotation on a reaction and the shape of the corresponding PES.

The prototypic H + H_2 reaction and its isotopic variants, for which the PES is known from *ab initio* calculations to a great accuracy,[23-25] provides a very good occasion for the investigation of the role of the different energy modes on the reaction dynamics. Previous QCT calculations have shown specifically that the total reaction cross section (σ_R) grows monotonically with both translational and vibrational energy in the postthreshold region[26-32] (at least up to $E_T \simeq 1$ eV), and that an increase in the rotational excitation of the H_2 molecule at low collision energies ($E_T \leqslant 0.6$ eV) leads to a minimum in σ_R.[33-35] Due to the mentioned accuracy in the knowledge of its PES, the H_3 system constitutes a unique ground for the comparison and experimental test of distinct theoretical approaches. The situation has become specially interesting in later times,[36,37] since the severe experimental difficulties associated with the study of the H + H_2 system at a detailed microscopic level are being gradually overcome and a wealth of experimental data is becoming available.[37-56] On the other hand, important progress in the methodology of quantum dynamical calculations has led to the extension of the pioneering exact 3D quantum scattering calculations by Schatz and Kuppermann[57] on H + H_2 to higher energies and to isotopic variants of the reaction.[58-74]

Specifically, for the D + H_2 reaction, the overall agreement between the theoretical calculations [exact quantum mechanical (QM)[59,68,69] and QCT[31,32,75]] and experimental measurements [which now include angle and velocity distributions from crossed molecular beams[42,45,46,48,55,56] as well as products' internal state distributions from coherent anti-Stokes Raman spectroscopy (CARS)[49,51] and resonantly enhanced multiphoton ionization (REMPI)[53,54] under single collision conditions] is good, but there exist some discrepancies. In particular, a detailed comparison between recent molecular beam differential cross sections (angle and velocity resolved) by Buntin, Giese, and Gentry[55] and by Contin-

 0021-9606/91/127991-17$03.00 © 1991 American Institute of Physics

This article is copyrighted as indicated in the article. Reuse of AIP content is subject to the terms at: http://scitation.aip.org/termsconditions. Downloaded to IP: 130.209.6.50 On: Fri, 19 Dec 2014 14:02:13

etti, Balko, and Lee[56] with the exact quantum mechanical results by Zhang and Miller[59] (on the LSTH surface[23]) and by Zhao, Truhlar, Schwenke, and Kouri[69] [on the double many body expansion (DMBE)[24] surface] for the $D + H_2 \rightarrow HD + H$ reaction, has apparently shown differences (the experiments indicate that the HD backward scattered products exhibit a higher rotational excitation than the theoretical predictions). This could suggest that some of the regions of the current potential energy surface might not be accurate enough. However, a very recent *ab initio* reevaluation of the H_3 potential,[25] specially of the bending configurations at high energies, has shown an excellent agreement with both the LSTH and the DMBE fits of previous *ab initio* points.

In former papers,[32,35] we have performed quasiclassical calculations of total and differential cross sections for the $D + H_2 \rightarrow HD + H$ system in a range of conditions of interest to recent experiments and for the comparison with exact QM results. In the present work, we extend our QCT study of the $D + H_2$ (v,j) reaction in order to systematically cover the $v = 0$–2, $j = 0$–12, and $E_T = 0.25$–1 eV intervals. This allows a consideration of the combined effects of translation, rotation, and vibration on reactivity. The relevance of QCT calculations is not only limited to the range of energies and angular momenta where exact QM calculations are not yet feasible or too cumbersome. It is also important to ascertain the validity of classical mechanics in predicting chemical attributes and to evince the appearance of specific quantum effects such as dynamical resonances.[50,51,72–74,76–79]

The present data might also be useful for future tests of the potential energy surface since they include a large set of initial conditions, many of them pertaining to those regions where the accuracy of the PES is not so firmly established.

II. QCT CALCULATION AND METHOD

The overall methodology followed in the present calculations is well described in the excellent reviews[26,80–82] available.

All the trajectories are calculated on the LSTH potential energy surface.[23] The integration of the differential set of equations of motion is carried out by using a Hamming predictor–corrector method with a fixed step size initialized by a fourth-order Runge–Kutta integration. Accuracy and stability in the integration is addressed in the usual way by checking the conservation of both total angular momentum and total energy. With a step size of 5×10^{-17} s, the conservation of total energy was invariably better than 1 in 5×10^6.

Calculations are carried out at selected E_T, v, and j values; namely, $v = 0$, 1, and 2 and E_T and j covering the ranges of 0.25–1.00 eV and of 0–12, respectively. The values of vibrorotational energies are calculated from the full Dunham expansion for H_2 for reactants and HD for products. Internal energy is deposited by placing the molecules at the beginning of the trajectory in alternatively the inner and outer turning points corresponding to the specific vibrorotational quantum numbers.

The rest of the initial conditions are sampled by an unbiased Monte Carlo method from the original distributions of the collision parameters.[80]

The maximum impact parameter is chosen such that no reactive trajectories are contained in the last few bins of the histogram of the opacity function, ranging from 0.7–2.0 Å depending on E_T, v, and j values. The initial reaction shell radius, i.e., the initial D–H_2 center-of-mass distance, is set in the interval of 5–6 Å depending on the phase of H–H vibrational motion.[26,80]

Assignation of final quantum numbers has been done by fitting the internal energy to the full Dunham expansion of vibrorotational energies of the HD molecule. The values v' and j' so obtained are rounded to the nearest integer, following the standard histogram method,[82,83] i.e., the probability for each reactive trajectory of having a quantum number n is $P_n(\nu) = 1$ if $n = n_c$ and $P_n(\nu) = 0$ if $n \neq n_c$, with n_c being the nearest integer to the real quantum number ν as calculated by the aforementioned procedure. Those trajectories yielding HD with vibrational energy between the minimum of the potential and $E(v' = 0)$ are taken as reactive with $v' = 0$.

The use of the quadratic smooth sampling method[82,83] to assign final quantum numbers does not produce any substantial change in values of the vibrationally state resolved cross section.

In the present as well as in former works,[32,35] the reactivity and final state functions are calculated by the method of moments expansion[80] in Fourier series.[84] This method has the advantage over the histogrammic one that it yields continuous functions describable by few coefficients and, therefore, much easier to handle. Legendre expansion[80] (or, for this respect, any other suitable expansion in orthogonal functions) is completely equivalent to the Fourier expansion here employed.

The opacity function $P_r(b)$ can be written in terms of the normalized function $G(\beta)$ as a cosine Fourier series

$$G(\beta) = \frac{\pi b^2_{\max}}{\sigma_R} P_r[b(\beta)] \sim 1 + \sum_{n=1}^{M} c_n \cos(n\pi\beta), \tag{1}$$

where $\beta \equiv b^2/b^2_{\max}$ is the unbiased sampling variable, with $b_{\max}$ being the limiting or maximum impact parameter.

The coefficients of the expansion (1) are given by[80,84]

$$c_n = \frac{2}{N_r} \sum_{i=1}^{N_r} \cos(n\pi\beta_i), \tag{2}$$

where the sum in Eq. (2) is upon the N_r reactive trajectories, each with $\beta_i = b^2_i/b^2_{\max}$, b_i being the impact parameter of the ith trajectory. Once the coefficients c_n are determined, the opacity function is given by

$$P_r(b) = \frac{\sigma_R}{\pi b^2_{\max}} G[\beta(b)]. \tag{3}$$

Several criteria have been used to truncate series (1) to M terms. The simplest one is to stop the expansion whenever the uncertainty γ_n (standard deviation, 68% confidence limit) of the coefficient c_n is of the order or less in absolute value than the c_n value itself. However, some of the c_n can be naturally small and the truncation would be incorrect. One means to avoid this is to compute the partial sums of the

This article is copyrighted as indicated in the article. Reuse of AIP content is subject to the terms at: http://scitation.aip.org/termsconditions. Downloaded to IP: 130.209.6.50 On: Fri, 19 Dec 2014 14:02:13

squares of the deviations of the c_n from γ_n, using as a stopping criterion the comparison of the successive partial sums with M and $M+1$ terms. The truncation takes place when these sums reach the same value.[84]

In the present work, the Smirnov–Kolmogorov statistical test[85] is employed as an additional stopping criterion. The number of coefficients is changed until the deviation of the observed and fitted cumulative probability distributions is small enough with a significance level of 70%–95%. This last criterion has proved to be very useful since the addition of more terms in the series (1) normally leads to a deterioration of the statistics due to the generation of noise.

The estimation of the error of the coefficients of the series is given by[84]

$$\gamma_n^2 \equiv \mathrm{var}(c_n) = \frac{4}{N_r}\mathrm{var}[\cos(n\pi\beta)] = \frac{1}{N_r}[4\langle\cos^2(n\pi\beta)\rangle - c_n^2], \tag{4}$$

where var ( ) refers to the variance and $\langle\ \rangle$ to the average over the ensemble of values of β_i from the N_r reactive trajectories. It can be shown that the upper limit of γ_n^2 is[84] $2/N_r$.

The error of the series $G(\beta)$ will then be given by

$$\mathrm{var}[G(\beta)] = \sum_{n=1}^{M}\left[\frac{\partial G(\beta)}{\partial c_n}\right]^2\gamma_n^2 = \sum_{n=1}^{M}\gamma_n^2[\cos(n\pi\beta)]^2. \tag{5}$$

Notice that the error will be maximum for $\beta = 0,1$ and minimum for $\beta = 1/2$, and that this error increases in general as the number of terms increases.

Finally, the statistical error ε (which will correspond to the 68% of significance level, provided that the number N_r is large enough) of the opacity function $P_r(b)$ will be given by

$$\varepsilon[P_r(b)] = \{\mathrm{var}[P_r(b)]\}^{1/2} \tag{6}$$

with

$$\begin{aligned}\mathrm{var}[P_r(b)] &= \mathrm{var}(\sigma_R)\left\{\frac{G[\beta(b)]}{\pi b_{\max}^2}\right\}^2 + \left(\frac{\sigma_R}{\pi b_{\max}^2}\right)^2\mathrm{var}\{G[\beta(b)]\} \\ &= [P_r(b)]^2\left(\frac{N-N_r}{N_rN}\right) + \left(\frac{\sigma_R}{\pi b_{\max}^2}\right)^2\sum_{n=1}^{M}\gamma_n^2\cos^2[n\pi\beta(b)].\end{aligned} \tag{7}$$

Figure 1(a) displays a comparison of the Fourier cosine expansion and the histogram method for the determination of the opacity function in three different cases. Following Ref. 80, the histogram bins are equally spaced in $\beta = b^2/b_{\max}^2$, rather than in b, since it is β the sampling variable. In this way, the total number of trajectories N_k in the k th bin, limited by (b_{k-1}, b_k), tends to be the same as for any other bin. The average value of the opacity function in this bin is[80]

$$\langle P_r(b)\rangle_k = \frac{N_{rk}}{N_k}, \tag{8}$$

where N_{rk} is the number of reactive trajectories in bin k.

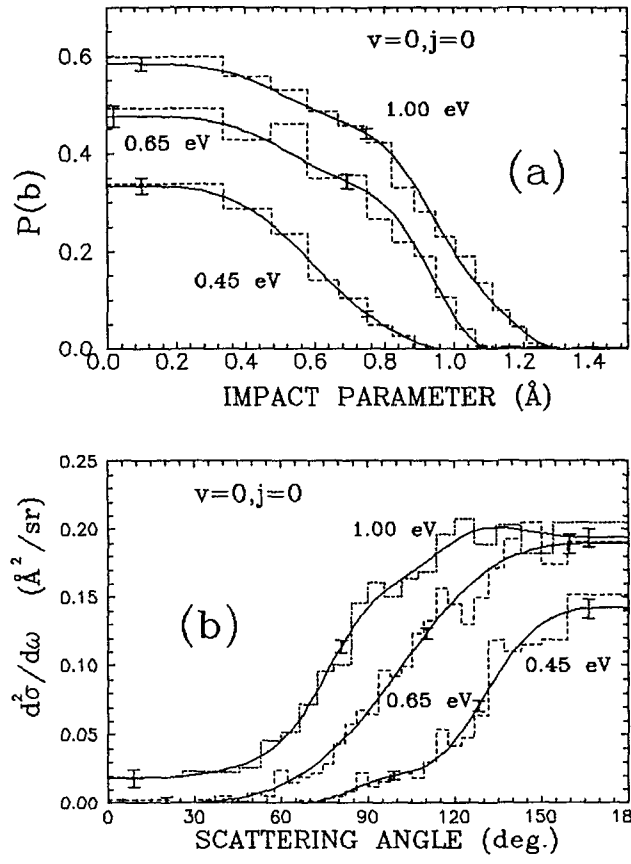

FIG. 1. Comparison of the Fourier moment expansion and the usual histogram methods for (a) opacity function $P(b)$ and (b) solid angle differential cross section. The figure shows the results at three different collision energies. The error bars in the Fourier fitting represent the uncertainty (68% confidence interval) calculated as described in the text. Note that the histograms are constructed following the uniform phase space criterion (Ref. 72) and accordingly the bins have equal size in $\beta = b^2/b_{\max}^2$ and in $\chi = 1/2(1-\cos\theta)$. The most probable errors in each bin are similar to error bars calculated for Fourier fits (see the text).

As can be seen, the agreement is excellent in all the cases. Error bars, calculated with expression (6), are shown at two values of b for each $P_r(b)$, to illustrate the uncertainty of the determination. The most probable error (68% confidence level) in any bin of the histogram is given by[80]

$$\varepsilon[\langle P_r(b)\rangle_k] = \frac{N_{rk}}{N_k}\left(\frac{N_k - N_{rk}}{N_kN_{rk}}\right)^{1/2}. \tag{9}$$

The uncertainties calculated by both methods are very similar.

When the statistical weight for different trajectories is not the same, for instance, when importance sampling[80] is used or when for final state resolved functions the quadratic smooth sampling is employed, function $G(\beta)$ becomes

$$G(\beta) = \frac{\pi b_{\max}^2}{\sigma_R}W(b)P_r[b(\beta)] \sim 1 + \sum_{n=1}^{M}c_n\cos(n\pi\beta) \tag{10}$$

and now the coefficients can be found as

$$c_n = \frac{2}{S_{N_r}}\sum_{i=1}^{N_r}W_i\cos(n\pi\beta_i) = 2\langle\cos n\pi\beta\rangle, \tag{11}$$

where

This article is copyrighted as indicated in the article. Reuse of AIP content is subject to the terms at: http://scitation.aip.org/termsconditions. Downloaded to IP: 130.209.6.50 On: Fri, 19 Dec 2014 14:02:13

$$\beta_i = \int_0^{b_i} P_r^0(b)\,\frac{2b}{b_{\max}}db = \int_0^{b_i}\frac{2b}{b_{\max}}\frac{db}{W(b)} \tag{12}$$

and

$$S_{N_R} = \sum_{i=1}^{N_R} W_i. \tag{13}$$

The sampling variable is now given by Eq. (12), where $P_r^0(b) \equiv 1/W(b)$ is the importance sampling function.[80]

The opacity function is given by

$$P_r(b) = \frac{\sigma_R}{\pi b_{\max}^2} P_r^0(b) G[\beta(b)] \tag{14}$$

with

$$\sigma_R = \frac{S_{N_r}}{\Sigma_{i=1}^{N} W_i}. \tag{15}$$

The statistical error of the opacity function (14) is obtained as in Eq. (6) with the variance being

$$\mathrm{var}[P_r(b)] = [P_r(b)]^2\left(\frac{N - S_{N_r}}{NS_{N_r}}\right) + \left[\frac{\sigma_R}{\pi b_{\max}^2} P_r^0(b)\right]^2 \times \mathrm{var}[G(\beta)]. \tag{16}$$

The var $[G(\beta)]$ is given by Eq. (5) and the error of the nth coefficient γ_n is now given by

$$\gamma_n = 4S_{N_r}^{-1}\mathrm{var}[\cos(n\pi\beta)] = S_{N_r}^{-1}[4\langle\cos^2(n\pi\beta)\rangle - c_n^2]. \tag{17}$$

A treatment entirely analogous holds for the representation of the solid angle differential cross section $d^2\sigma_R/d\omega$. In this case, the adequate variable is chosen to fulfill the criterion of "uniform phase space" (see Ref. 80), i.e.,

$$\chi = 1/2(1 - \cos\theta), \tag{18}$$

where θ is the scattering angle with respect to the direction of the incoming atom. The variable χ is bounded in [0,1]. The solid angle differential cross section is, in terms of the normalized function $g(\chi)$, also expanded in cosine series

$$\frac{d^2\sigma_R}{d\omega} = \frac{\sigma_R}{4\pi} g(\chi) = \frac{\sigma_R}{4\pi}\left[1 + \sum_{n=1}^{M} a_n \cos(n\pi\chi)\right]. \tag{19}$$

The coefficients are given as in Eq. (2)

$$a_n = \frac{2}{N_r}\sum_{i=1}^{N_r}\cos(n\pi\chi_i). \tag{20}$$

The same truncation criteria applied in series (1) are valid for Eq. (19).

The statistical error (68% confidence level) of the solid angle differential cross section is the square root of its variance given by

$$\mathrm{var}\left(\frac{d^2\sigma_R}{d\omega}\right) = \left(\frac{d^2\sigma_R}{d\omega}\right)^2\left[\frac{N - N_r}{NN_r} + \frac{\Sigma_{n=1}^{M}\gamma_n^2\cos^2(n\pi\chi)}{|g(\chi)|^2}\right], \tag{21}$$

where γ_n, the uncertainties of the coefficients, are given by the equivalent to expression (4).

Figure 1(b) represents the $d^2\sigma_R/d\omega$ for the same three cases as Fig. 1(a). The curves are the cosine expansions. Their statistical uncertainties at three values of θ are shown in each case. The same figure contains the corresponding histograms built with bins equally spaced in χ. Again, the agreement is excellent with similar uncertainties in both cases, but with the advantage, in the case of the continuous curves, of being describable by less data. When state resolved differential cross sections are calculated, the sums in Eq. (20) are restricted to those reactive trajectories which yield products at the indicated quantum number. If quadratic smooth sampling (or importance sampling) is used, analogous expressions to Eqs. (11) and (17) will hold for the coefficients a_n and their uncertainties γ_n, respectively.

For the continuous probability functions of the translational and rotational fractions of the total energy available to the products, the same method has been employed. Instead of a cosine series, a sine series could be used, especially when the function to be expanded becomes null in $x = 0$ and $x = 1$. In some cases, a smoothing procedure could be convenient (see Ref. 84).

The total number of calculated trajectories relevant to this work has been 950 000.

III. RESULTS AND DISCUSSION

A. Total reaction cross section

The absolute values of the total reaction cross section $\sigma_R(v,j,E_T)$ for the D + H_2 → HD + H system as a function of translational, rotational, and vibrational energy are shown in Figs. 2–8 and their values are listed systematically in Table I.

The behavior of the reaction cross section as a function of rotational energy is portrayed in Fig. 2 for the three first vibrational states of the H_2 molecule and at several collision energies. Undoubtedly, the most salient feature is the presence of a minimum in the dependence of σ_R with E_R at low collision energies, say, below 0.65 eV. This effect has already been shown in previous calculations carried out on the H_3 system for H_2 ($v = 0$)[33] and H_2($v = 1$).[34,35] Present work shows that such a minimum, at j values between $j = 4$–6, exists even when the molecule is in its $v = 2$ level.

For all three vibrational quantum numbers studied here, the minimum gets gradually more shallow with increasing E_T and eventually disappears at a collision energy of ~0.65 eV, as first shown by Boonenberg and Mayne[33] in their QCT calculations for the H + H_2($v = 0$) reactive system. At the collision energy of 1 eV, σ_R increases monotonically with E_R. As can be seen, the decrease in absolute value of σ_R in the region where the minimum exists is more pronounced in going from $v = 0$ to $v = 2$. However, this representation could be misleading. In fact, the *relative* decrease in reactivity associated with this minimum becomes less prominent with increasing vibrational quantum number of H_2. This is clearly shown in Fig. 3, where the $\sigma_R(j,v)/\sigma_R(j = 0,v)$ values for each vibrational number as a function of the H_2 rotational quantum number are displayed at 0.35 and 0.45 eV of collision energy. It is apparent that the relative decrease is more dramatic for $v = 0$ than for $v = 1$ and $v = 2$. At 0.35 eV, the cross section in $v = 0$ is, at the minimum, 5% of that for $j = 0$, whereas it is 80% in the case of $v = 2$. It is interesting to note how the relative minimum shifts toward higher values of j in going from $v = 0$ to $v = 2$.

This article is copyrighted as indicated in the article. Reuse of AIP content is subject to the terms at: http://scitation.aip.org/termsconditions. Downloaded to IP: 130.209.6.50 On: Fri, 19 Dec 2014 14:02:13

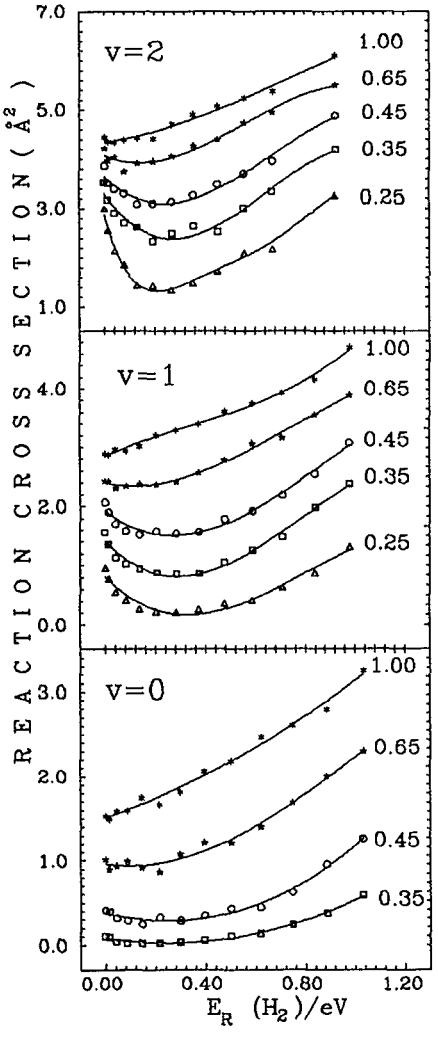

FIG. 2. Total reaction cross section (in Å^2) for the D + H$_2$(v,j) → HD + H system as a function of H$_2$ rotational energy (eV) at the indicated translational energies (0.25, 0.35, 0.45, 0.65, and 1.00 eV) and for the three first H$_2$ vibrational levels $v=0$ (lower panel), $v=1$ (middle panel), and $v=2$ (upper panel). Errors in σ_R (68% standard deviation) are of the order or smaller than the size of the represented points (see Table I). The lines through the points are polynomial fittings to the points.

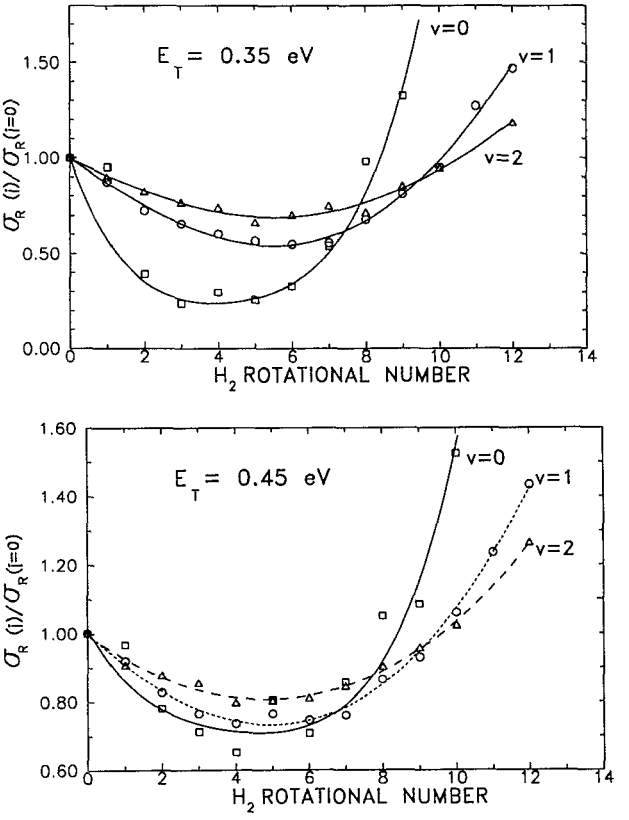

FIG. 3. The ratio of $\sigma_R(j,v)/\sigma_R(j=0,v)$ vs the H$_2$ rotational quantum number for $v=0$ (squares), $v=1$ (circles), and $v=2$ (triangles). (a) At 0.35 eV; (b) at 0.45 eV. The lines through the points are error weighted least-squares fits.

The subsequent rise after the minimum is also steeper for $v=0$ than for $v=1$ and $v=2$. The j value where the cross section equals that of $j=0$ goes from $j=8$ at $v=0$, $E_T=0.35$ eV, to $j=10$ for $v=2$. The same effects can be observed at 0.45 eV of collision energy [Fig. 3(b)], although to a lesser extent, reflecting the fact already stated that translational energy tends to smooth and cancel the negative effect of rotational energy in the cross section.

In terms of the translational energy, the cross section grows monotonically from a threshold dependent on v and j, and tends to level off at high values (>1 eV) of the collision energy as shown in Figs. 4–8. Increasing the vibrational quantum number of the H$_2$ molecule also causes a monotonic increase in σ_R. For a given j, and for values of E_T away enough from threshold, vibration is more efficient than translation in promoting the reaction under study, as can be seen in Fig. 7, where σ_R is represented as a function of total energy. The opposite is true in the vicinity of the threshold. This effect was already observed in a QCT study of H + H$_2$($j=0$) by Barg, Mayne, and Toennies.[30]

The present results are in good agreement (mostly within experimental error) with the total cross section values obtained from the existing experiments with microscopic resolution for D + H$_2$($v=0$)[38,49] and D + H$_2$($v=1$).[46]

QCT total cross-section values for this reaction had been calculated previously at some of the collision energies

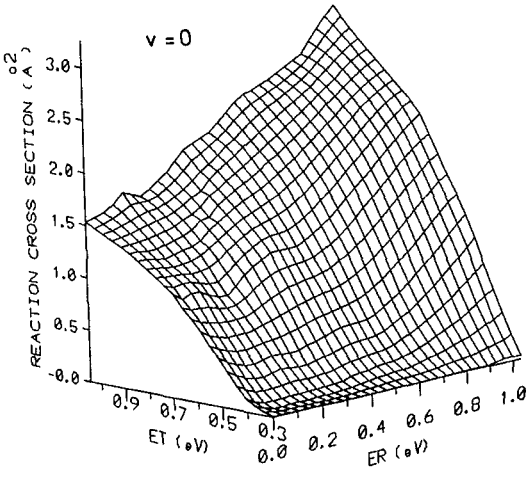

FIG. 4. A 3D plot of the reaction cross section (in Å^2) as a function of translational E_T and rotational energy E_R in (eV) for the H$_2$ vibrational quantum number $v=0$.

This article is copyrighted as indicated in the article. Reuse of AIP content is subject to the terms at: http://scitation.aip.org/termsconditions. Downloaded to IP: 130.209.6.50 On: Fri, 19 Dec 2014 14:02:13

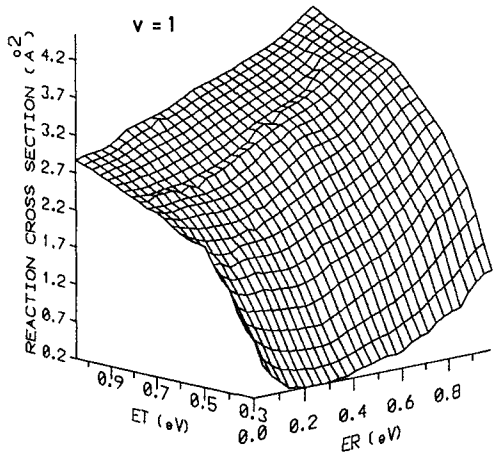

FIG. 5. The same as Fig. 4 for $v = 1$.

considered here, especially for $v = 0$ (Refs. 31 and 75) and in some cases for $v = 1$ (Refs. 31, 34, and 68). The agreement is, in general, good, but there is a discrepancy, greater than the statistical error, between present values and those of Ref. 31 in the results for $v = 1$ at E_T above 0.45 eV. This is probably due to the fact that in Ref. 31, and only for $v = 1$, those trajectories with vibrational energies below the products' zero point energy have been considered as nonreactive (see above). In the present work, such a criterion has not been used in any case.

Recently, exact quantum mechanical results[59,69] have also yielded values of $\sigma_R(E_T)$ over a wide range of translational energies. Due to practical difficulties, the quantum mechanical calculations are limited to low values of the rotational quantum number of the H_2 molecule.

There is a remarkable general concordance between the QCT results and exact quantum mechanical ones, not only in the total cross sections, but also in more detailed reactivity functions and product state distributions as already discussed in previous work.[32,67]

Figure 8 displays a detailed comparison of QM $\sigma_R(E_T)$ values from Refs. 59 and 69 and present QCT results. As can be seen, the agreement for $v = 0$ is better at low translational

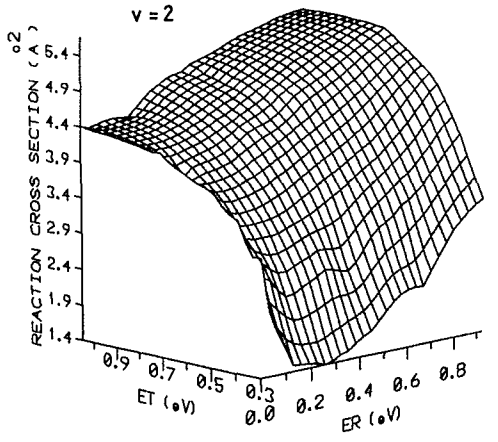

FIG. 6. The same as Fig. 5 for $v = 2$.

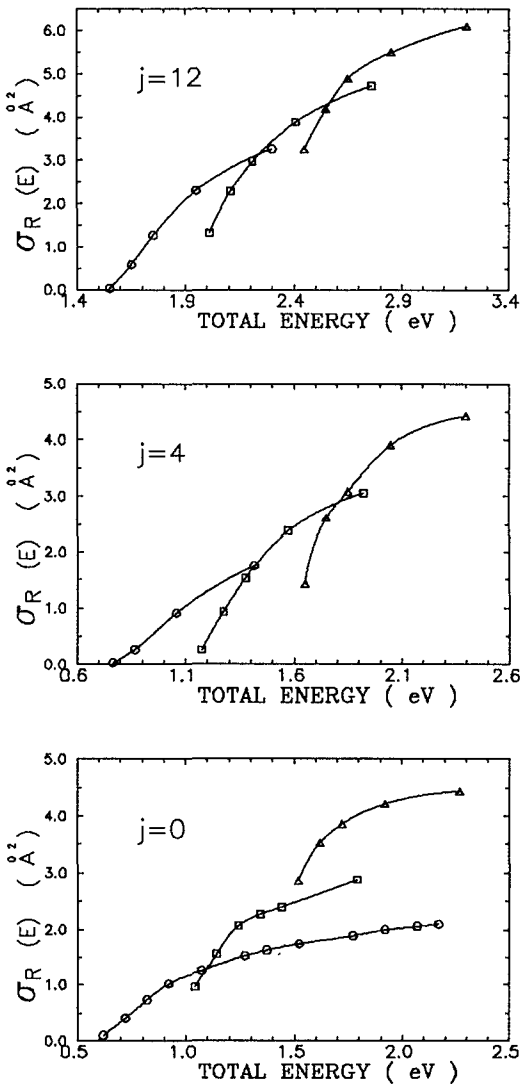

FIG. 7. The reaction cross section (in Å^2) vs total energy for specific values of v ($v = 0$, circles; $v = 1$, squares; $v = 2$, triangles) and j ($j = 0$ lower; $j = 4$ middle; $j = 12$ upper panel) for the D + $H_2(v,j)$ → HD (all) + H reaction.

energies. At energies above 0.6 eV, QM results are systematically larger. The slight differences between the two QM calculations[59,69] are probably due to the different potential energy surfaces used. For the reaction with $v = 1$, the concordance between QCT and QM is even better at total energies comparable to those of the $v = 0$ case. A similar agreement between QCT and QM results has been reported very recently by Zhao *et al.*[70] for the H + D_2 isotopic analog of this reaction.

Several numerical models of varying complexity have been developed in an attempt to relate the reactivity attributes observed in the reactions of the $A + BC$ type to the main topological features of the corresponding potential energy surface. Most of these models extend the original considerations of Polanyi about the steric requirements imposed on the dynamics by the PES.

The familiar line-of-centers model[86] has been often invoked to explain the rise in $\sigma_R(E_T)$ characteristic of reactions with a threshold; in fact, a modified line-of-centers

This article is copyrighted as indicated in the article. Reuse of AIP content is subject to the terms at: http://scitation.aip.org/termsconditions. Downloaded to IP: 130.209.6.50 On: Fri, 19 Dec 2014 14:02:13

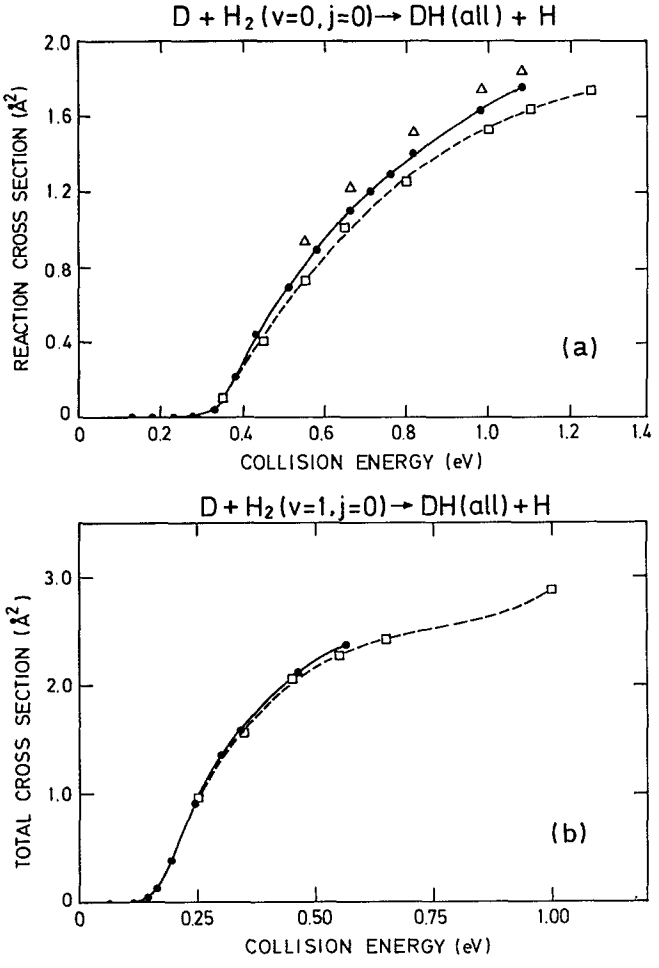

FIG. 8. A comparison of the total reaction cross section from QM accurate calculations and QCT present results (a) for $v = 0, j = 0$ and (b) for $v = 1$, $j = 0$. Symbols: open squares, dashed line this work; closed circles, solid line from Ref. 57 (on the LSTH surface); open triangles (for $v = 0$), Ref. 63 (on the DMBE surface).

model which includes the dependence of the barrier height on the relative orientation of the colliding partners[87,88] was applied to the H_3 system by Levine and Bernstein,[88] who calculated the excitation function $H + D_2$ $(v = j = 0) \rightarrow HD + D$ and compared their results with the trajectory calculations by Blais and Truhlar.[89] The agreement is very good at low energies, but the model calculations yield a slightly larger cross section than the QCT for the highest collision energy compared (1.30 eV). In a recent work on $D + H_2$,[32] we have observed a similar deviation between the model calculations and the QCT results for translational energies beyond approximately 0.8 eV. The deviation grows with increasing collision energy and has been attributed by Levine[22] to recrossing of trajectories from the products to the reactants valley. The recrossing mechanism would thus be responsible for the leveling off in the excitation function of $D + H_2$ obtained in trajectory calculations.[42] A postthreshold rise similar to the one described is observed in our calculations (see Table I) for all the cases studied, the threshold being dependent on the particular v,j case. The modified "line-of-centers" model can also account reasonably well for the evolution of the opacity function with growing collision energy: increase of $P(b)$ (for all b) and of the "cut-off" b value (the maximum impact parameter for which reaction takes place) (see Figs. 9–11). The model gives a simple expression for the "cone of acceptance" (i.e., the range of orientations that can lead to reaction), but does not include rotation or reorientation effects during the collision.

Due to the symmetry of the PES of this system, the energy barrier to reaction is placed in the middle of the way from the reactants' to the products' valley. It is therefore interesting to consider the effects of vibration on the cross section, since in this case, the simple rationalizations mentioned in the introduction for reactions with an "early" and a "late" barrier do not apply.

The opacity functions of Figs. 9–11 as well as those from former trajectory calculations[30] for the H_3 system show that vibrational excitation of the molecule enhances the reactivity for each impact parameter and enlarges the range of impact parameters that lead to reaction. In their trajectory study of $H + H_2(v)$, Barg, Mayne, and Toennies[30] discuss both effects and indicate that vibrational excitation results in an increase of the zero point energy, which, for a given impact parameter, widens the range of configurations of the three atoms that can lead to reaction. They further stress the fact that vibrational energy is perpendicular to the reactant channel, and once the saddle point has been reached, it should be more effective than translation in promoting reaction. The authors also suggest that reorientation effects tending to align the molecular axis with the direction of the incoming atom could be important near threshold. The fact that larger impact parameters lead to reaction with increasing v is attributed by the authors to the larger amplitude of the vibrational motion that increases the anisotropy and thus the orienting character of the potential.

Levine[22,90] and co-workers have also analyzed the enhancement of the cross section for this reaction caused by vibrational excitation and have traced it back to the steric requirements imposed by the PES. The main effect of vibration would be to lower the angle-dependent barrier to reaction. In the spirit of the modified line-of-centers model commented above, a lowering of the angle-dependent barrier $E_0(\gamma)$ leads to an increase in the cross section for any given initial orientation (angle of attack[88]) and to a wider range of initial orientations that can contribute to reaction. This opening up of the cone of acceptance upon vibrational excitation predicted by the model and verified by trajectory calculations of Schechter *et al.*[90] for $D + H_2(v)$ and $H + D_2(v)$, results both in a larger $P(b)$ at each b and in a larger range of reactive impact parameters with growing vibrational excitation of the molecule as indeed observed (see Figs. 9–11).

Schechter *et al.*[90] also mention trajectory computations which would show that translational and vibrational excitations produce a similar enhancement in the cross section for this reaction. This may be the case at some energies, but away enough from threshold vibration is more efficient than translation in promoting the reaction as shown in the work of Barg, Mayne, and Toennies[30] and in Fig. 7 of the present

This article is copyrighted as indicated in the article. Reuse of AIP content is subject to the terms at: http://scitation.aip.org/termsconditions. Downloaded to IP: 130.209.6.50 On: Fri, 19 Dec 2014 14:02:13

TABLE I. Total reaction cross sections σ_R (in Å^2) for the D + $H_2(v,j) \rightarrow$ HD + D reaction as a function of collision energy and of the initial rotational and vibrational quantum numbers of the H_2 molecule. Values in parentheses represent the 68% statistical confidence level.

		E_T (eV)									
		0.25		0.35		0.45		0.65		1.00	
v	j										
0	0			0.102	(0.005)	0.410	(0.016)	1.014	(0.030)	1.525	(0.021)
0	1			0.097	(0.013)	0.396	(0.018)	0.898	(0.030)	1.487	(0.041)
0	2			0.040	(0.010)	0.320	(0.010)	0.938	(0.029)	1.581	(0.034)
0	3			0.024	(0.001)	0.292	(0.014)	0.994	(0.037)	1.590	(0.050)
0	4			0.023	(0.006)	0.267	(0.014)	0.910	(0.050)	1.745	(0.051)
0	5			0.026	(0.004)	0.330	(0.020)	0.870	(0.050)	1.672	(0.070)
0	6			0.034	(0.002)	0.290	(0.015)	1.080	(0.060)	1.816	(0.078)
0	7			0.055	(0.007)	0.351	(0.020)	1.220	(0.060)	2.064	(0.058)
0	8			0.100	(0.020)	0.430	(0.040)	1.219	(0.055)	2.188	(0.073)
0	9			0.135	(0.007)	0.445	(0.014)	1.400	(0.060)	2.472	(0.060)
0	10			0.240	(0.030)	0.625	(0.019)	1.692	(0.044)	2.608	(0.076)
0	11			0.374	(0.019)	0.908	(0.026)	2.000	(0.071)	2.794	(0.102)
0	12	0.030	(0.010)	0.590	(0.040)	1.260	(0.060)	2.299	(0.062)	3.249	(0.095)
1	0	0.979	(0.015)	1.558	(0.032)	2.037	(0.028)	2.425	(0.033)	2.880	(0.036)
1	1	0.780	(0.030)	1.360	(0.044)	1.900	(0.050)	2.420	(0.070)	2.870	(0.100)
1	2	0.559	(0.024)	1.130	(0.033)	1.707	(0.068)	2.310	(0.070)	2.958	(0.078)
1	3	0.410	(0.026)	1.020	(0.032)	1.578	(0.046)	2.340	(0.080)	2.940	(0.100)
1	4	0.246	(0.006)	0.936	(0.021)	1.520	(0.039)	2.380	(0.080)	3.047	(0.078)
1	5	0.226	(0.020)	0.880	(0.037)	1.580	(0.066)	2.375	(0.075)	3.198	(0.120)
1	6	0.212	(0.020)	0.855	(0.030)	1.540	(0.065)	2.410	(0.080)	3.283	(0.079)
1	7	0.260	(0.018)	0.865	(0.052)	1.570	(0.066)	2.562	(0.080)	3.400	(0.100)
1	8	0.360	(0.025)	1.056	(0.028)	1.787	(0.034)	2.770	(0.080)	3.608	(0.109)
1	9	0.410	(0.040)	1.260	(0.060)	1.920	(0.070)	3.060	(0.090)	3.746	(0.110)
1	10	0.629	(0.037)	1.480	(0.037)	2.190	(0.073)	3.156	(0.078)	3.930	(0.130)
1	11	0.870	(0.050)	1.980	(0.071)	2.550	(0.076)	3.556	(0.079)	4.157	(0.120)
1	12	1.320	(0.050)	2.289	(0.037)	2.962	(0.049)	3.880	(0.090)	4.712	(0.090)
2	0	2.995	(0.066)	3.525	(0.063)	3.860	(0.075)	4.212	(0.077)	4.375	(0.068)
2	1	2.550	(0.100)	3.170	(0.090)	3.510	(0.130)	3.960	(0.140)	4.343	(0.120)
2	2	2.137	(0.055)	2.900	(0.070)	3.390	(0.120)	4.026	(0.134)	4.338	(0.120)
2	3	1.840	(0.070)	2.704	(0.060)	3.300	(0.120)	3.740	(0.140)	4.383	(0.120)
2	4	1.430	(0.060)	2.612	(0.060)	3.080	(0.120)	3.910	(0.130)	4.422	(0.130)
2	5	1.430	(0.070)	2.336	(0.096)	3.100	(0.120)	3.950	(0.110)	4.410	(0.130)
2	6	1.340	(0.099)	2.480	(0.070)	3.130	(0.100)	4.040	(0.126)	4.694	(0.130)
2	7	1.492	(0.064)	2.640	(0.076)	3.262	(0.110)	4.260	(0.140)	4.900	(0.150)
2	8	1.710	(0.070)	2.520	(0.110)	3.484	(0.130)	4.390	(0.130)	5.070	(0.130)
2	9	2.090	(0.070)	3.010	(0.080)	3.695	(0.110)	4.720	(0.130)	5.230	(0.130)
2	10	2.170	(0.130)	3.330	(0.120)	3.950	(0.130)	4.940	(0.140)	5.360	(0.130)
2	12	3.250	(0.110)	4.180	(0.130)	4.880	(0.140)	5.492	(0.136)	6.090	(0.140)

work.

The mentioned line-of-centers model could also help to understand the different efficiency of vibration and translation in promoting the reaction. The application of the model to the opacity functions of Figs. 9–11 would yield values of the translational threshold $E_0(\gamma = 0)$ and of the hard-sphere diameter D that decrease and increase, respectively, with growing v. In fact, the actual potential barrier is higher for larger internuclear distances (larger D), but vibrational energy is used to surmount the barrier. The net effect is that the translational threshold gets smaller with vibrational excitation, but does not disappear even for $v = 2$. It is the persistence of this translational threshold which makes the cross section smaller for the higher vibrational levels at the same total energy and low E_T (see Fig. 7). The rotational excitation of the H_2 molecule does not modify this effect. At higher collision energies, vibrational excitation, which implies as indicated lower $E_0(\gamma = 0)$ and higher D, would lead to larger σ_R.

A very interesting effect also pointed out by Levine and co-workers and related to the vibrational excitation in this reaction is the appearance, upon vibrational stretching of the molecule, of a well in the potential for a collinear configuration, best seen in a $V(R,\gamma)$ representation[90] (where R is the distance of the attacking atom to the center of mass of the molecule and γ the angle of attack). Levine and Wu[78(a)] suggested that this well should give rise to resonances[76–79] in the reaction dynamics. These resonances, though present in 3D quantum mechanical calculations for the lowest partial waves,[66] do not show up in the recent exact QM calculations,[59,69] at least in the integral cross section.[73,74] Results initially interpreted as giving evidence of the mentioned resonances[50] are being now reconsidered.[36,37]

The effects of rotational excitation on the total reaction

This article is copyrighted as indicated in the article. Reuse of AIP content is subject to the terms at: http://scitation.aip.org/termsconditions. Downloaded to IP: 130.209.6.50 On: Fri, 19 Dec 2014 14:02:13

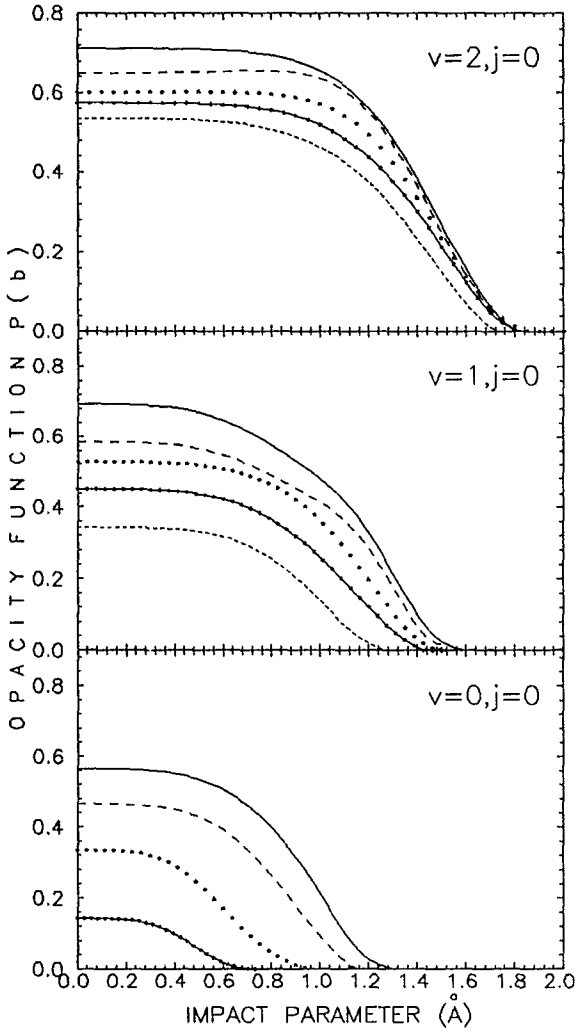

FIG. 9. Opacity function $P(b)$ for the D + H_2 ($v,j=0$) → HD (all) + H at several translational energies: small dashes, $E_T = 0.25$ eV; dotted line, $E_T = 0.35$ eV; dots, $E_T = 0.45$ eV; dashed line, $E_T = 0.65$ eV; solid line, $E_T = 1.00$ eV. Lower panel, $v = 0$; middle, $v = 1$; upper, $v = 2$. Typical error bars (not shown) are the same as in Fig. 1(a).

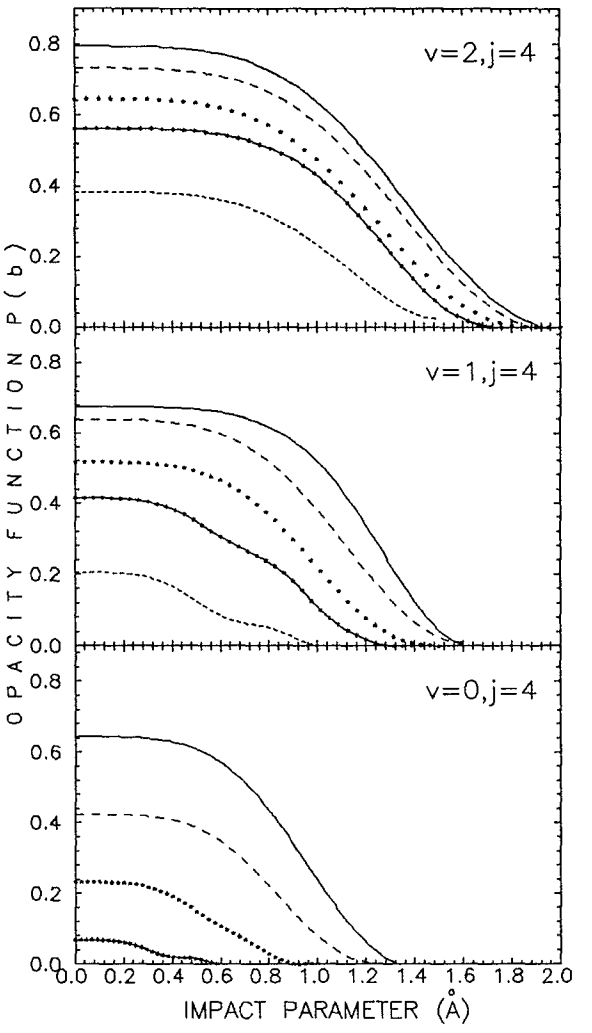

FIG. 10. The same as Fig. 8 for the D + H_2 ($v,j=4$) → HD (all) + H.

cross section for reactions of an atom with a diatomic molecule have also deserved much attention. For the H + $H_2(j)$ system, the fact that rotational excitation can inhibit reactivity was already noticed in the pioneering QCT calculations by Karplus, Porter, and Sharma[26] who found that the threshold in the translational excitation function increased with growing j. They interpreted this fact as due to the decrease of the "orienting effect" (which would drive the system to a collinear configuration) of the surface at higher j. Polanyi and co-workers[91] gave a qualitative explanation of the minimum in the rotational excitation function $\sigma_R(E_R)$, present in this and other systems, in terms of two competing effects: the "orientation" effect (responsible for the decrease and present at low j) and the "energy" effect, which would cause the increase in $\sigma_R(E_R)$ observed for high values of j, i.e., higher values of the total energy.[6] The orientation effect mentioned has indeed been shown in pictorial representations of trajectories.[92]

Simplifying models like the modified line of centers one commented on before do not account for any reorientation of the colliding partners during the collision. It was thus necessary to develop more complex treatments in order to unveil the key features of the influence of rotational excitation on reactivity. These models imply the solution of the classical equations of motion with some dimensionality reducing approximations.

In particular, Loesch[13,14] proposed a rotational sliding mass model for reactions of the $A + BC(j)$ type, where BC is treated as a rigid rotor and only collisions with zero impact parameter are considered. This model was successfully tested against trajectory calculations on different surfaces and made possible, in the reactions analyzed, to establish a relationship between the shape of $\sigma_R(E_R)$ and the anisotropic attributes (steric restrictions) of the potential energy surface. The approaching molecules experience torques caused by the mentioned anisotropy of the potential which can direct them, either away from or toward the favored geometry for reaction, thus defining a dynamical cone of acceptance distinct from the static one. In that respect, both the decline and the rise in $\sigma_R(E_R)$ would be at least in some cases the result of a more general orientation effect. In a later treat-

This article is copyrighted as indicated in the article. Reuse of AIP content is subject to the terms at: http://scitation.aip.org/termsconditions. Downloaded to IP: 130.209.6.50 On: Fri, 19 Dec 2014 14:02:13

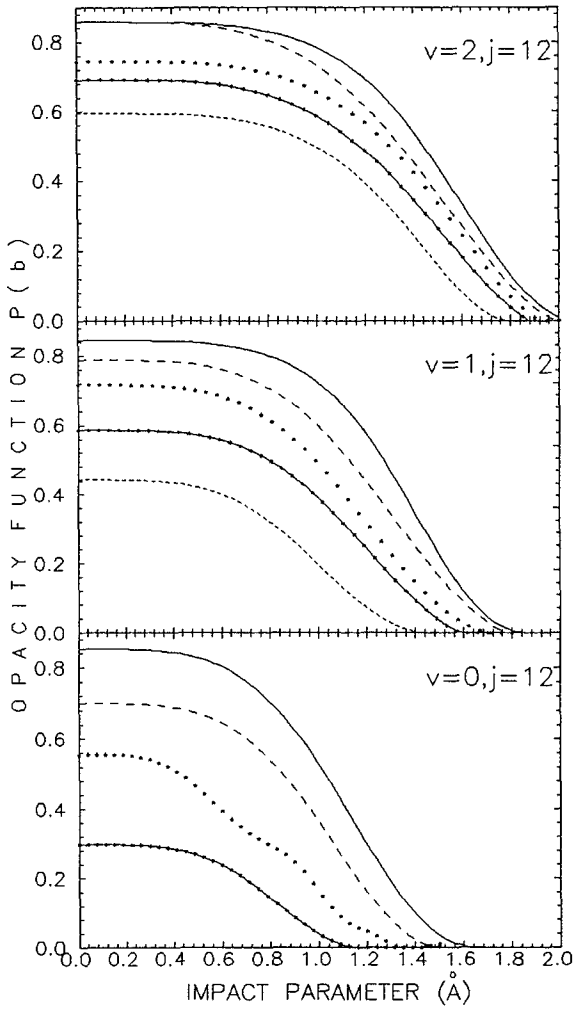

FIG. 11. The same as Fig. 8 for the D + H_2 ($v_j = 12$) → HD (all) + H.

ment, Grote *et al.*[7] also included the energy effect and obtained the rise observed in $\sigma_R(j)$ for H + $H_2(j)$ for $E_T > 0.65$. Their results compare very well with the QCT calculations by Boonenberg and Mayne.[33]

Mayne and co-workers[15–19] have also developed a model similar to that of Loesch but with some differences: instead of considering *BC* as a rigid rotor, the bond length is allowed to vary adiabatically.[15] The variation of the molecule's bond length leads to a changing moment of inertia which couples explicitly rotational energy to translational motion and was found necessary[16] in order to reproduce the increase in $\sigma_R(E_R)$ observed in the trajectory calculations for H + $H_2(j)$ at high j.[33] The model was later refined to treat nonzero impact parameters and was applied to the collisions of two diatomic molecules.[17] Recently, Harrison and Mayne,[19] in an attempt to further clarify the effects of rotational excitation on reactivity, have compared the results of two decoupling approximations: the "classical centrifugal sudden" (CSS) approximation, which assumes that the dynamical variable l (orbital angular momentum) can be replaced by a constant value, and the "classical infinite order sudden" (CIOS) approximation, which in addition to the simplification contained in CCS, makes the "energy sudden" approximation forcing $d\gamma/dt = 0$ (where γ is the orientation angle) during the collision. They performed total cross section calculations on a model system (not intended to fit any particular real system) and found that CCS was in very good qualitative agreement with the exact QCT calculations carried under the same conditions for all the mass combinations and translational energies they tried. The CIOS approximation, which by definition forbids the mixing of γ motion and motion along the reaction coordinate, was unable to reproduce the minima observed in $\sigma_R(E_R)$ (i.e., the orientation effect) and could only account for the increase in $\sigma_R(E_R)$ associated with the "energy" effect.

Levine and co-workers[20–22] have also attributed the effects of rotation on total cross sections to dynamical reorientation of the reagents on the way to the barrier. They use the j_z conserving approximation, the $V(R,\gamma)$ potential and discuss the reorientation in terms of the "physical" and the "chemical" shape of the molecule, as seen by the approaching atom. The physical shape is given by the equipotential contours which determine how close the atom can get to the molecule at a given collision energy. Usually, a closer approach is possible from certain directions, and in that case, the *ABC* system is said to be "oblate" if *A* can get closer to *BC* when $\gamma = 0°$ as compared with $\gamma = 90°$, ($\cos\gamma = \hat{R}_{BC}\hat{R}_{A,BC}$) and "prolate" for the opposite case. The chemical shape is defined by the location of the barrier to reaction. They show that for systems with an oblate physical shape (as is the case for H + H_2) in the absence of molecular rotation, the forces outside the barrier tend to steer the reagents into the cone of acceptance; initial rotation would hinder this steering, leading thus to a decline in $\sigma_R(E_R)$. The enhancement of the total cross section with rotational excitation is attributed to the anisotropy in the location of the chemical barrier.[22]

Although the reducing dimensionality models just commented on differ in the details of their formulation and have often been tested against distinct reactions, they all share the central idea that dynamical reorientation caused by the anisotropy of the potential in the course of the reactive encounter is responsible for most of the observed effects of rotational excitation on reactivity.

In the spirit of these models, the more stringent the steric hindrances for a process and the closer the collision energy to the threshold for reaction, the more marked should be the effect of rotation on reactivity.

This is in qualitative agreement with the results of the present and previous calculations (see Table I and Figs. 2–6).

However, to the best of our knowledge, no numerical model results have been reported that reproduce the minimum in $\sigma_R(E_R)$ for this concrete reaction on its well known potential energy surface.

B. Differential cross section and energy distribution among the reaction products

The dependence of the (c.m.) solid angle differential cross section on the translational, rotational, and vibrational energies of the reactants is depicted in Figs. 12–14. In most of the cases studied, the HD product is scattered predomi-

This article is copyrighted as indicated in the article. Reuse of AIP content is subject to the terms at: http://scitation.aip.org/termsconditions. Downloaded to IP: 130.209.6.50 On: Fri, 19 Dec 2014 14:02:13

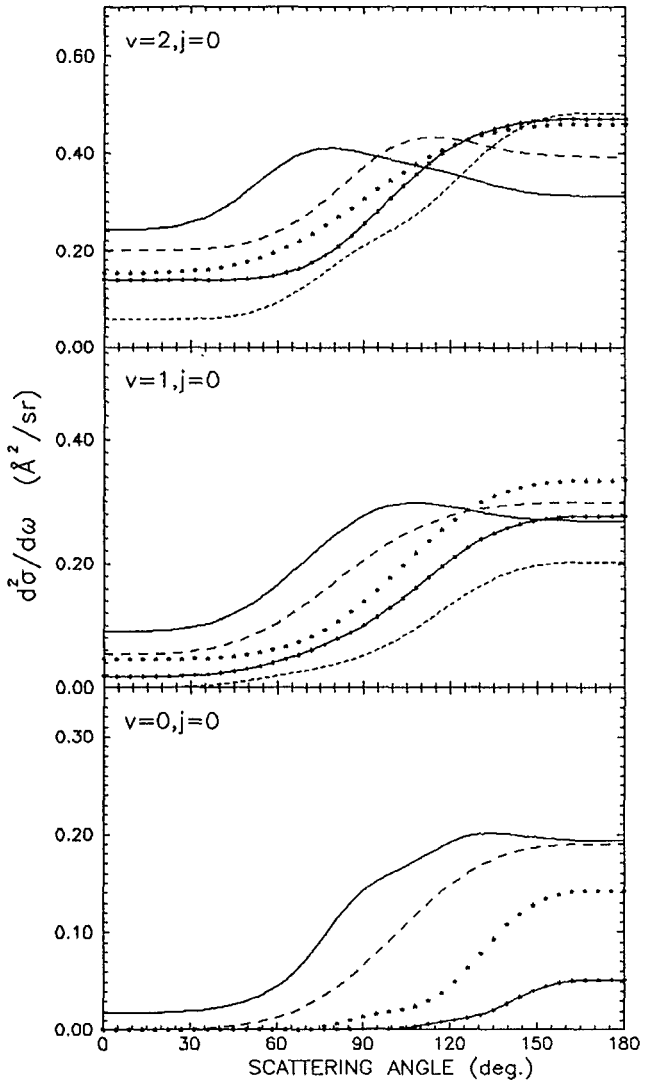

FIG. 12. The solid angle differential cross section summed over all v' and j' final states for the D + H_2 ($v,j=0$) → HD + H at several translational energies: small dashes, 0.25 eV; dotted line, $E_T = 0.35$ eV; dots, $E_T = 0.45$ eV; dashed line, $E_T = 0.65$ eV; solid line, $E_T = 1.00$ eV. Lower panel, $v = 0$; middle, $v = 1$; upper, $v = 2$. Uncertainties, not shown for clarity, are similar to those of Fig. 1(b) (see text).

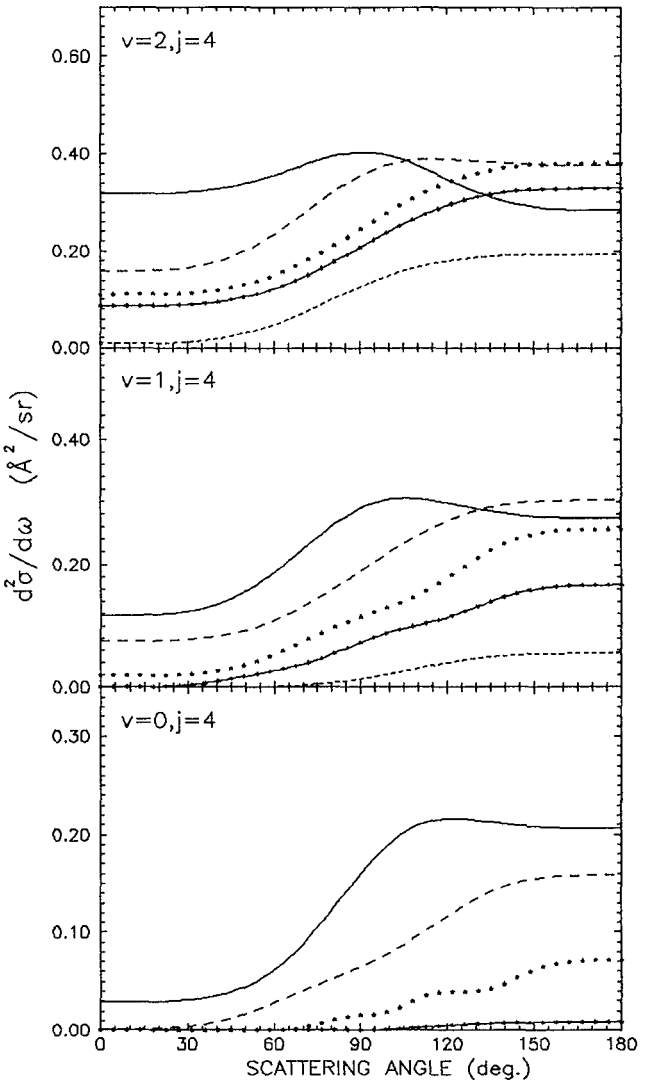

FIG. 13. The solid angle differential cross section for the D + H_2 ($v,j=4$) → HD + H reaction. Symbols are the same as in Fig. 12.

nantly in the backward hemisphere with respect to the direction of the incoming D atom. Many of the angular distributions shown have a maximum at 180°. An increase in the collision energy (with v and j fixed) leads to wider and more forward angular distributions. The same effect is observed with growing vibrational quantum number for a given E_T and j. The differential cross sections for the $j=4$ case [which corresponds approximately to the minimum in $\sigma_R(j)$ present at low E_T] are shown in Fig. 13. Such a moderate increase in the rotational energy does not greatly change the shape of the angular distributions for the higher collision energies, but has a noticeable effect for the lower values ($E_T < 0.65$). A comparison of Figs. 12 and 13 and of the corresponding opacity functions (Figs. 9 and 10) shows that the initial decrease in $\sigma_R(j)$ happens mainly for collisions with low impact parameters, which seem to correlate with backward scattered HD product. A comparison between Figs. 9–11 and 12–14 also shows a relationship between forward scattering and collisions with high impact parameter. In general, the forward character of the angular distribution increases markedly in the cases where $P(b)$ extends beyond $b \simeq 1.2$ Å. Maxima of the angular distributions at c.m. angles clearly distinct from 180° are obtained just for values of the total energy higher than 2 eV.

Some of the present angular distributions can be compared to other theoretical calculations for D + H_2($v=0,1$) → HD + H already mentioned in the discussion of the total cross section. The agreement with existing QCT results is very good.[34,42,75]

Our differential cross sections from Fig. 12 show the same trend as the recent QM exact results by Zhang and Miller[59] (for $v=0,1; j=0$) and by Zhao *et al.*[69] (for $v=0$; $j=0,1$) except for the forward peak at the highest translational energies, which is unseen in our results, and for the already commented absolute value of the reaction cross section. A more detailed comparison between QCT and exact

This article is copyrighted as indicated in the article. Reuse of AIP content is subject to the terms at: http://scitation.aip.org/termsconditions. Downloaded to IP: 130.209.6.50 On: Fri, 19 Dec 2014 14:02:13

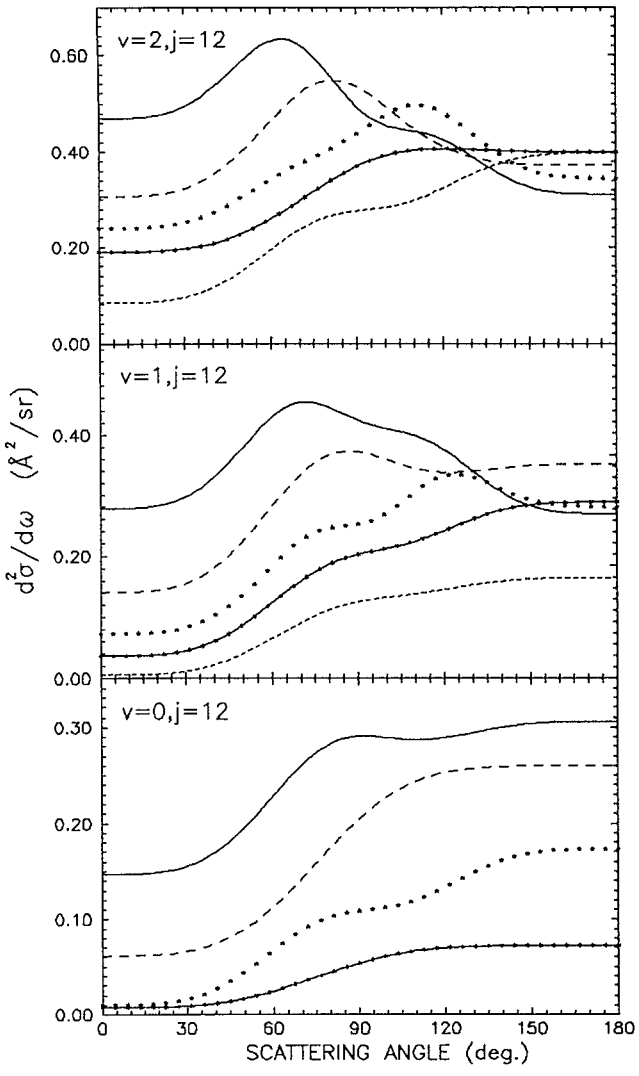

FIG. 14. The solid angle differential cross section for the D + H_2 ($v_j = 12$) → HD + H reaction. Symbols are the same as in Fig. 12.

quantum mechanical vibrational state resolved angular distributions for $v = 0$ was reported in previous work.[32]

Simple models have also been applied to calculate the differential reaction cross section of the system under study. Kwei and Herschbach[93] showed by means of an optical model that a hard-sphere deflection function directly relating scattering angle and impact parameter could account for the angular distributions obtained by Schatz and Kupperman[57] for the H + H_2 ($v = 0$) reaction at low collision energies. A hard-sphere deflection function was also used by Götting *et al.*[42] in the frame of an impulsive line-of-centers model with an angle-dependent barrier of the type commented above.[88] The model, restricted to coplanar collisions, yielded c.m. differential cross sections which compare reasonably well with the QCT ones used by the same authors in order to reproduce their experimental results on D + H_2 ($v = 0$) at an average collision energy of 1.5 eV. In particular, the tendency to more sidewards and forward scattering with increasing collision energy is rendered by the model. The major discrepancy lies in the products velocity distributions, which are predicted to be narrower than those from the QCT. If the orientation dependence of the barrier is not contemplated, the model velocity distributions differ considerably (being broader and greater) from the experimental ones.[42]

The simple arguments contained in the mentioned models can probably account for the translational energy dependence of the c.m. angular distributions of Fig. 12 of the present work, not only for D + H_2 ($v = 0$), but also for the reaction with $v = 1$ and $v = 2$.

The partition of the available energy among the products' degrees of freedom is represented in Figs. 15–20 and in Table II. Figures 15–17 show the dependence of the average translational ($\overline{E}'_T$), rotational ($\overline{E}'_R$), and vibrational ($\overline{E}'_v$) energy of the products on the translational, rotational, and vibrational excitations of the reactants. The probability density functions of the fractions of rotation (f'_R) and translation (f'_T) of the products are depicted in Figs. 18–20. Table II lists the cross sections for the production of HD in a given vibrational state v'.

An inspection of Figs. 15–17 reveals some interesting

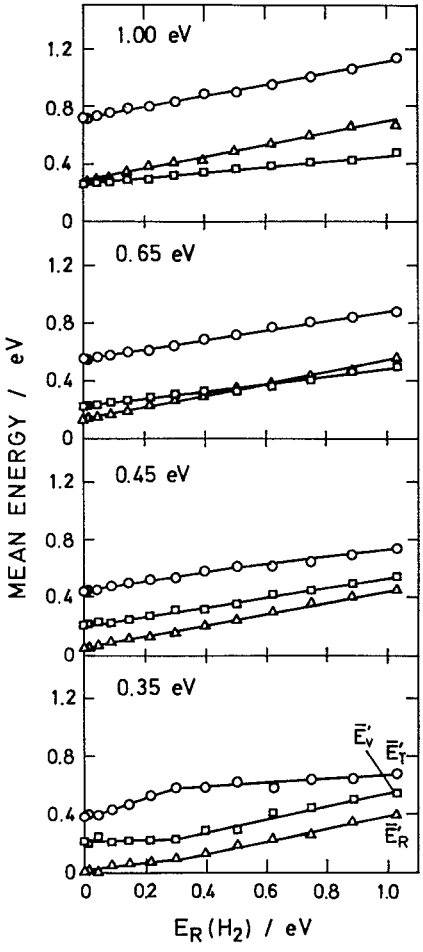

FIG. 15. Average values of the products' translational $\overline{E}'_T$ (circles), rotational $\overline{E}'_R$ (triangles), and vibrational $\overline{E}'_v$ (squares) energy vs the H_2 rotational energy for the D + H_2 ($v = 0$) → HD + H reaction at several collision energies (top left-hand corner in each box). All the units in electron-volts.

This article is copyrighted as indicated in the article. Reuse of AIP content is subject to the terms at: http://scitation.aip.org/termsconditions. Downloaded to IP: 130.209.6.50 On: Fri, 19 Dec 2014 14:02:13

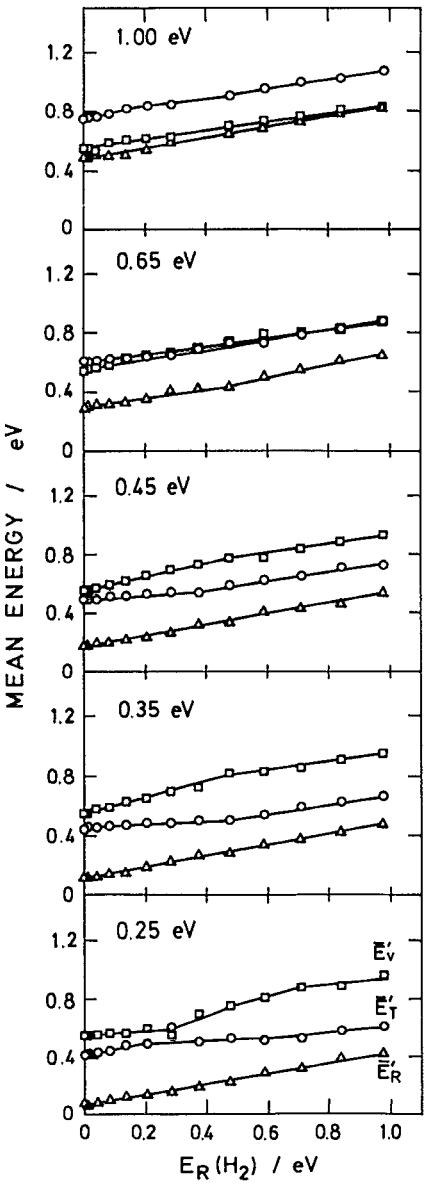

FIG. 16. The same as Fig. 15, but for the D + H_2 ($v = 1$) → HD + H reaction.

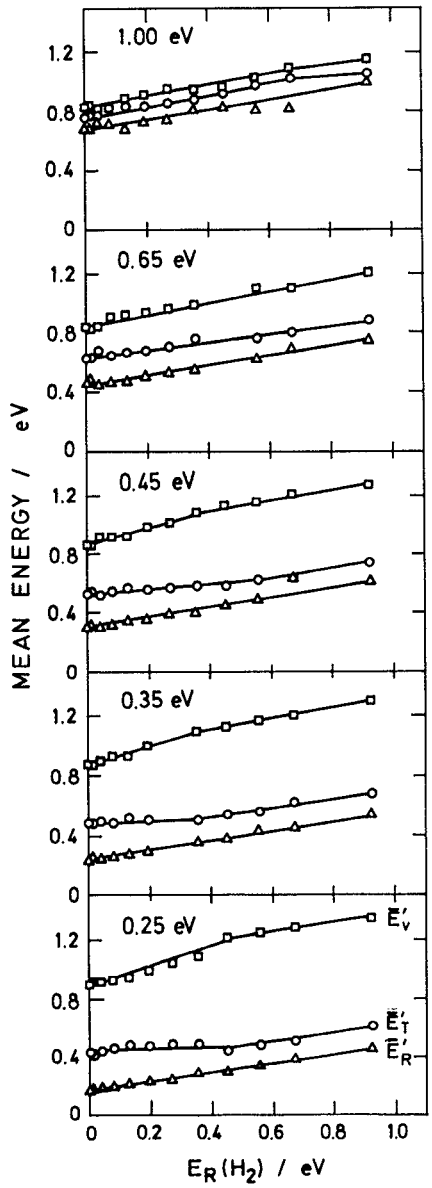

FIG. 17. The same as Fig. 15, but for the D + H_2 ($v = 2$) → HD + H reaction.

features that should be stressed. Although in all the cases considered there is a certain degree of interconversion between the reactants' and products' energy modes, most of the translational excitation of the reactants appears as translational energy in the products and the same is also true for the vibrational excitation. In fact, the average translational energy of the products does not depend at all on the vibrational quantum number of H_2, and the average vibrational energy of the HD product is nearly independent of the collision energy. These general assertions need, however, some precisions. Part of the vibrational energy (E_v) of the H_2 molecule goes always to the other products modes (E'_T and E'_R) in collisions with low E_T and low E_R. In the $v = 2$ case, $\overline{E}'_v$ decreases somewhat with increasing E_T, especially for the higher j. On the other hand, the average translational energy of the reactants $\overline{E}'_T$ is higher than the collision energy for low E_T and low j. This is no longer the case with growing collision energy. Increasing either the translational or the vibrational energy of the reactants leads always to an increase in the rotational energy of the products.

The initial rotation of the H_2 molecule goes to all three products' modes as is apparent from Figs. 15–17. In all cases, $\overline{E}'_R$ grows linearly with E_R. At the lower collision energies, there is an E_R range, corresponding to the region around the minimum in $\sigma_R(j)$ (see Figs. 2 and 3) for which $\overline{E}'_T$ remains nearly constant with increasing E_R as already commented on in previous work.[35] For higher j and for higher translational energies, both $\overline{E}'_T$ and $\overline{E}'_v$ also grow linearly with E_R. In any case, the fraction of energy appearing as products' rotation is relatively low (always less than one third). This suggests that rotational excitation of H_2 is efficient for the promotion of the reaction under study as far as it can be converted to a significant extent into translational or vibrational energy in the course of the reactive encounter.

This article is copyrighted as indicated in the article. Reuse of AIP content is subject to the terms at: http://scitation.aip.org/termsconditions. Downloaded to IP: 130.209.6.50 On: Fri, 19 Dec 2014 14:02:13

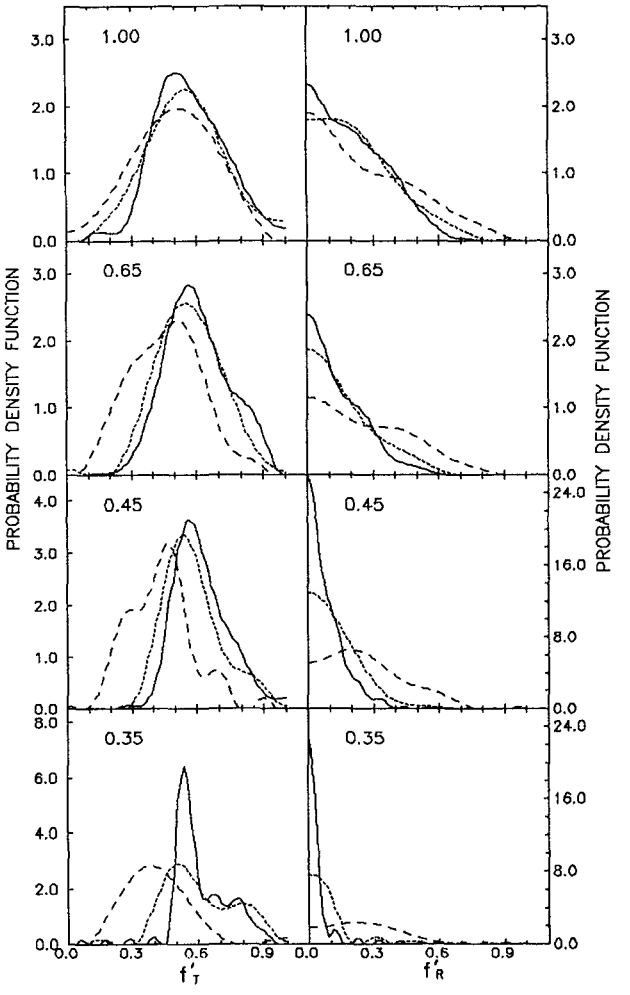

FIG. 18. Probability density functions of the translational f'_T (left) and rotational f'_R (right) fractions of the total energy available to the products for the D + H_2 ($v = 0$) → HD + H reaction. Solid line, $j = 0$; small dashes, $j = 4$; large dashes, $j = 12$. The collision energies are indicated in the upper left-hand corner of each box. The "fast oscillations" in some of the curves are probably an artifact of the fitting and lie within the calculated uncertainty.

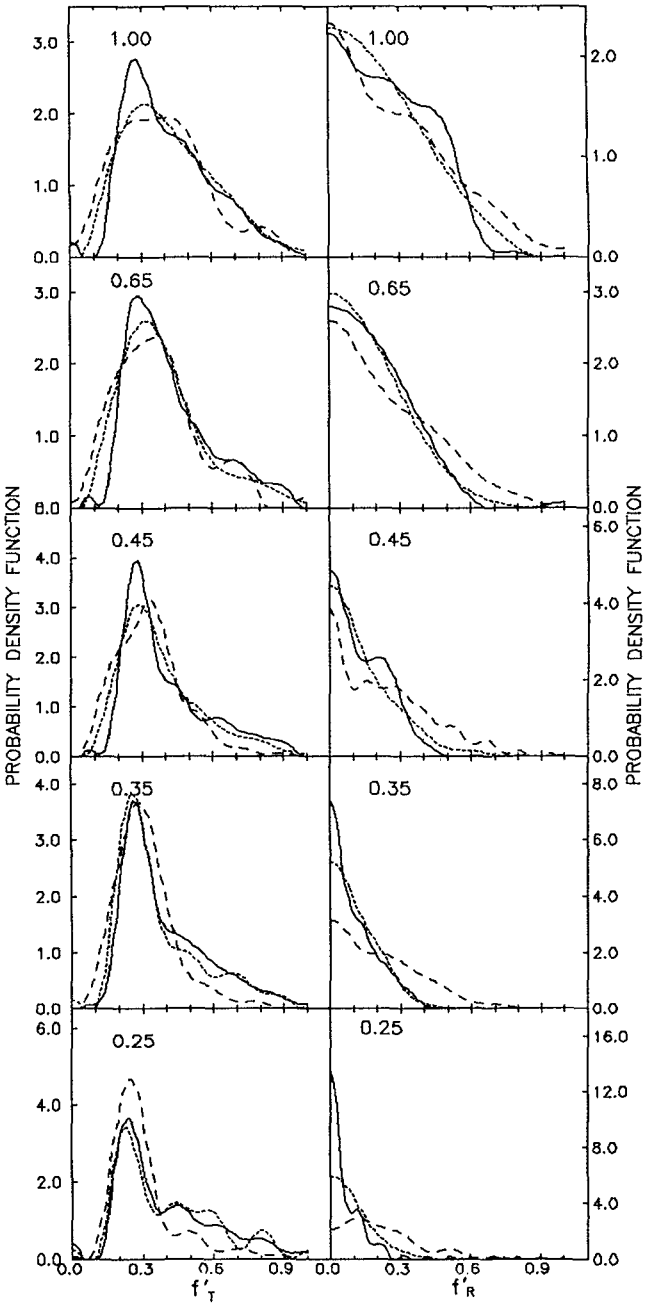

FIG. 19. The same as Fig. 18 for the D + H_2 ($v = 1, j$) → HD (all) + H reaction.

The products' translational distributions represented as $P(f'_T)$ in Figs. 18–20 are clearly asymmetric for low E_T and j with a definite peak at relatively low f'_T and a long tail extending to higher f'_T. In the $v = 0$ case, an increase in the translation or rotation of the reactants makes the $P(f'_T)$ distributions broader and more symmetric. For $v = 1$ and $v = 2$, the $P(f'_T)$ distributions also become broader, especially with growing E_T, and the peak shifts to lower f'_T. The asymmetry remains here over the range of conditions studied. The distributions of rotational energy in the products $P(f'_R)$ are much more sensitive to the variation of E_T and E_R than to the vibrational quantum number of H_2. The $P(f'_R)$ distributions always widen markedly with increasing collision energy. For the lower E_T, these distributions broaden significantly with j; however, for the higher values of the initial translational energy, the shape of $P(f'_R)$ does not change much with growing j.

The relative populations of the HD vibrational levels that can be deduced from Table II also become broader with any increase in the energy of the reactants, irrespective of the mode E_T, E_R, E_v, in which this energy is localized. For the lower E_T and the lower j, the reaction is predominantly adiabatic in the vibrational quantum number. The most populated product vibrational state shifts to higher v' with increasing j and to lower v' with growing E_T.

The general good concordance, with small differences, between the cross sections for the production of a given vibrational state σ_R ($v, j = 0 \rightarrow v'$) given by QCT and by recent exact QM calculations[59,69] was already commented on in a previous work[32] for $v = 0$. A similar agreement is obtained between the present results and those by Zhang and Miller[59]

This article is copyrighted as indicated in the article. Reuse of AIP content is subject to the terms at: http://scitation.aip.org/termsconditions. Downloaded to IP: 130.209.6.50 On: Fri, 19 Dec 2014 14:02:13

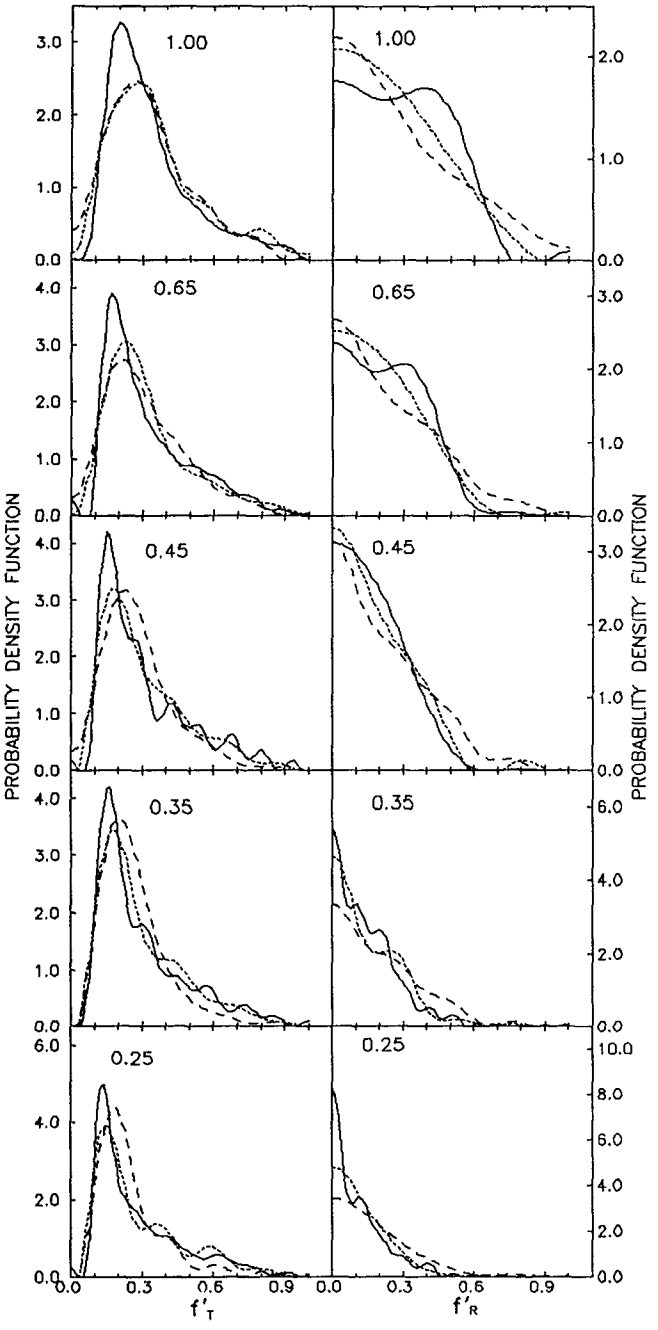

FIG. 20. The same as Fig. 18 for the D + H_2 ($v = 2j$) → HD (all) + H reaction.

for $v = 1$ at low collision energies. The QCT cross sections for $v = 1 \rightarrow v' = 0$ are nearly identical to the QM ones, whereas those for $v = 1 \rightarrow v' = 1$ are slightly smaller.

The most interesting result of the present work concerning the redistribution of the reagents' specific excitation (E_T, E_R, E_v) among the different products' energy modes is probably the relatively large degree of "adiabaticity" with respect to translation and vibration. A possible explanation for it has been given in a qualitative picture by Polanyi upon consideration of collinear trajectories on a potential surface with a barrier. According to this explanation, translational excitation in excess of the barrier height ΔE_T should give rise to a more compressed intermediate configuration, which is more repulsive and would lead to enhanced products' translation $\Delta E'_T$. On the contrary, a corresponding increase in vibrational excitation ΔE_v would lead most often to more extended intermediate configurations, smaller repulsion, and enhanced product vibration. These effects were termed, respectively, "induced repulsive energy release" ($\Delta E_T \rightarrow \Delta E'_T$) and "induced attractive energy release" ($\Delta E_v \rightarrow \Delta E'_v$).[91] If one takes into account the fact that with increasing collision energy more bent configurations become accessible for reaction, and that collisions with bent configurations lead more easily to rotational excitation, one can write[1] $\Delta E_T \rightarrow \Delta E'_T + \Delta E'_R$. By the same reasoning, an excess in vibrational energy also widens the acceptance cone (see above) and consequently gives rise to an increase in rotational excitation $\Delta E_v \rightarrow \Delta E'_R$. In fact, all the qualitative trends just described are present in the results of this work (see Figs. 15–17).

IV. SUMMARY AND CONCLUSIONS

Classical trajectory calculations have been carried out to study the D + H_2 (v,j) → HD + H reaction dynamics. The influence of translational, rotational, and vibrational energies of the reactants has been investigated by running QCT trajectories on the LSTH potential energy surface in the range of collision energy from 0.25 to 1 eV, H_2 rotational quantum number up to 12, and vibrational quantum number $v = 0$, 1, and 2. Total integral and differential cross sections, as well as the disposal of energy among the products' degrees of freedom, have been investigated.

Both translational and vibrational excitation of the reactants produce a monotonic increase in the total reaction cross section. For values of the total energy away enough from threshold, vibration is more efficient in promoting the reaction.

For the three vibrational numbers studied, the rotational excitation functions show a minimum at the lower collision energies at $j \simeq 4$–6. This minimum disappears with increasing translational energy and its relative depth decreases with growing v.

The center-of-mass angular distributions of the scattered HD are predominantly backward at low energies, with a maximum at 180° with respect to the direction of the incoming D atom, but they broaden considerably and become more forward with increasing total energy. The distributions of energy in the different products' modes also broaden markedly with growing energy. It is significant that translational and vibrational energies are largely adiabatic with respect to each other, while rotational energy interconverts more efficiently with the other two modes in the course of reactive collisions.

Although a detailed comparison between classical and quantum results is not the main aim of this work, it should be noted that with the level of resolution of the present QCT calculations (which implies summation at least over the products' rotational quantum numbers), the agreement with QM exact data is fairly good with slight differences; this

This article is copyrighted as indicated in the article. Reuse of AIP content is subject to the terms at: http://scitation.aip.org/termsconditions. Downloaded to IP: 130.209.6.50 On: Fri, 19 Dec 2014 14:02:13

TABLE II. Total reaction cross sections (in Å^2) for the D + $H_2(v,j) \rightarrow HD(v')$ + H at several collision energies (E_T). Values in parentheses are standard deviations of the last digit.

		$v=0$			$v=1$			$v=2$		
E_T (eV)	v'	$j=0$	$j=4$	$j=12$	$j=0$	$j=4$	$j=12$	$j=0$	$j=4$	$j=12$
0.25	0				0.295(9)	0.078(3)	0.19(2)	0.40 (3)	0.22(3)	0.35(4)
	1				0.680(1)	0.151(5)	0.22(2)	0.76 (4)	0.29(3)	0.23(3)
	2				0.005(1)	0.017(2)	0.70(6)	1.67 (5)	0.77(5)	0.48(5)
	3						0.20(2)	0.17 (2)	0.16(2)	1.33(8)
	4									0.85(6)
	5									0.02(1)
	6									
0.35	0	0.102(5)	0.030(3)	0.20(3)	0.48 (2)	0.21 (1)	0.30(2)	0.51 (3)	0.39 (3)	0.33(5)
	1			0.36(3)	1.05 (3)	0.63 (2)	0.52(2)	1.00 (4)	0.60(3)	0.45(5)
	2			0.03(1)	0.032(5)	0.09 (1)	1.16(3)	1.77 (5)	1.24(5)	0.94(7)
	3						0.30(2)	0.24 (2)	0.39(3)	1.55(9)
	4									0.88(7)
	5									0.03(1)
0.45	0	0.41 (2)	0.27 (1)	0.41(4)	0.64 (2)	0.38 (2)	0.42(3)	0.600(3)	0.50(5)	0.43(5)
	1	0.003(1)	0.002(1)	0.80(5)	1.28 (2)	0.98 (3)	0.83(4)	1.210(5)	0.74(7)	0.66(6)
	2			0.05(1)	0.115(8)	0.17 (1)	1.36(5)	1.680(6)	1.38(9)	1.31(9)
	3						0.45(3)	0.370(3)	0.47(5)	1.40(9)
	4						0.02(1)			0.94(7)
	5									0.13(3)
0.65	0	0.95 (3)	0.85 (5)	1.10(5)	0.88 (3)	0.66 (5)	0.69(5)	0.86 (4)	0.60(6)	0.68(6)
	1	0.069(8)	0.06 (1)	1.02(5)	1.32 (3)	1.39 (7)	1.28(7)	1.31 (5)	1.11(8)	0.85(7)
	2			0.18(2)	0.20 (1)	0.33 (4)	1.30(7)	1.65 (6)	1.55(9)	1.39(8)
	3						0.57(4)	1.39 (3)	0.64(6)	1.48(9)
	4						0.04(1)		0.02(1)	0.85(7)
	5									0.22(3)
	6									0.02(1)
1.00	0	1.28 (2)	1.45 (5)	1.74(5)	1.28 (3)	1.16 (6)	1.19(5)	0.85 (3)	0.89(7)	1.04(7)
	1	0.236(9)	0.27 (2)	1.16(7)	1.17 (3)	1.30 (6)	1.45(6)	1.68 (5)	1.41(8)	1.10(8)
	2	0.010(2)	0.03 (1)	0.26(3)	0.37 (1)	0.47 (4)	1.30(5)	1.28 (4)	1.35(8)	1.26(8)
	3			0.07(2)	0.066(6)	0.12 (2)	0.52(4)	0.46 (3)	0.58(6)	1.25(8)
	4						0.21(2)	0.10 (1)	0.17(3)	0.92(7)
	5						0.04(1)		0.03(1)	0.31(4)
	6									0.11(2)

good agreement, already shown in former works for $v=0$, is demonstrated here for the $v=1$ case. Where they can be compared, our results also show a general good concordance with previous QCT calculations and lie mostly within experimental error.

It is also interesting to observe that not only classical mechanics, but also very simple models can render, sometimes in a semiquantitative way, many of the dynamical characteristics of the reaction. Particularly successful have been hard-sphere models with an angle-dependent barrier in order to rationalize the effects of translation and vibration on total cross sections and angular distributions. Hard-sphere models are not sufficient to account for the role of rotation on the reactivity and it has been necessary to develop more complex treatments that consider explicitly a dynamical reorientation of the reactants in the course of the collision.

ACKNOWLEDGMENTS

This work was financed in part by the CICYT of Spain under Grants PB 870263 and PB 890041. The authors wish to thank Professor R. D. Levine and Dr. H. R. Mayne for their valuable comments about the results of this article.

[1] J. C. Polanyi, Agnew. Chem. Int. Ed. Eng. **26**, 952 (1987) (Nobel Lecture) and references cited therein.
[2] J. C. Polanyi and J. L. Schreiber, in *Physical Chemistry—An Advanced Treatise*, edited by H. Eyring, W. Jost, and D. Henderson (Academic, New York, 1974), Vol. VI A and references cited therein.
[3] (a) M. G. Ding, L. J. Kirsch, D. S. Perry, J. C. Polanyi, and J. L. Schreiber, Faraday Discuss Chem. Soc. **55**, 252 (1973); (b) J. C. Polanyi, *ibid.*, **55**, 389 (1973).
[4] R. D. Levine and R. B. Bernstein, *Molecular Reaction Dynamics and Chemical Reactivity* (Oxford University, New York, 1987).
[5] A. González Ureña, Adv. Chem. Phys. **66**, 214 (1987).
[6] N. Sathyamurthy, Chem. Rev. **83**, 601 (1983).
[7] W. Grote, M. Hoffmeister, R. Schleysing, H. Zerhau-Dreihöfer, and H. J. Loesch, in *Selectivity in Chemical Reactions*, edited by J. C. Whitehead (Kluwer, Dordrecht, 1988).
[8] S. R. Leone, Annu. Rev. Phys. Chem. **35**, 109 (1984).
[9] J. Wolfrum, in *Selectivity in Chemical Reactions*, edited by J. C. Whitehead (Kluwer, Dordrecht, 1988).
[10] P. J. Kuntz, E. M. Nemeth, J. C. Polanyi, S. D. Rosner, and C. E. Young, J. Chem. Phys. **44**, 1168 (1966).
[11] D. G. Truhlar and D. A. Dixon, in *Atom–Molecule Collision Theory: a Guide for the Experimentalist*, edited by R. B. Bernstein (Plenum, New York, 1979).
[12] J. C. Polanyi and W. H. Wong, J. Chem. Phys. **51**, 1439 (1969).
[13] H. J. Loesch, Chem. Phys. **104**, 213 (1986).
[14] H. J. Loesch, Chem. Phys. **112**, 85 (1987).
[15] H. R. Mayne, Chem. Phys. Lett. **130**, 249 (1986).
[16] H. R. Mayne and S. Minick, J. Phys. Chem. **91**, 1400 (1987).
[17] J. A. Harrison and H. R. Mayne, J. Chem. Phys. **88**, 7424 (1988).
[18] J. A. Harrison, L. J. Isakson, and H. R. Mayne, J. Chem. Phys. **91**, 6906 (1989).

This article is copyrighted as indicated in the article. Reuse of AIP content is subject to the terms at: http://scitation.aip.org/termsconditions. Downloaded to IP: 130.209.6.50 On: Fri, 19 Dec 2014 14:02:13

[19]J. A. Harrison and H. R. Mayne, Chem. Phys. Lett. **158**, 356 (1989).
[20]H. Kornweitz, A. Persky, and R. D. Levine, Chem. Phys. Lett. **128**, 443 (1986).
[21]H. Kornweitz, A. Persky, I. Schechter, and R. D. Levine, Chem. Phys. Lett. **169**, 489 (1990).
[22]R. D. Levine, J. Phys. Chem. **94**, 8872 (1990).
[23](a) P. Siegbahn and B. Liu, J. Chem. Phys. **68**, 2457 (1978); (b) D. G. Truhlar and C. J. Horowitz, *ibid.* **68**, 2466 (1978); **71**, 1514E (1979).
[24]A. J. C. Varandas, F. B. Brown, C. A. Mead, D. G. Truhlar, and N. C. Blais, J. Chem. Phys. **86**, 6258 (1987).
[25]C. W. Bauschlicher, Jr., S. R. Langhoff, and H. Partridge, Chem. Phys. Lett. **170**, 345 (1990).
[26]M. Karplus, R. N. Porter, and R. D. Sharma, J. Chem. Phys. **43**, 3259 (1965).
[27]V. I. Osherov, V. G. Ushakov, and L. A. Lomakin, Chem. Phys. Lett. **55**, 513 (1978).
[28]H. R. Mayne, Chem. Phys. Lett. **66**, 487 (1979).
[29]H. R. Mayne and J. P. Toennies, J. Chem. Phys. **70**, 5314 (1979).
[30]G. D. Barg, H. R. Mayne, and J. P. Toennies, J. Chem. Phys. **74**, 1017 (1981).
[31]H. R. Mayne and J. P. Toennies, J. Chem. Phys. **75**, 1794 (1981).
[32]F. J. Aoiz, V. Candela, V. J. Herrero, and V. Sáez Rábanos, Chem. Phys. Lett. **169**, 243 (1990).
[33]C. A. Boonenberg and H. Mayne, Chem. Phys. Lett. **108**, 67 (1984).
[34]N. Sathyamurthy and J. P. Toennies, Chem. Phys. Lett. **143**, 323 (1988).
[35]F. J. Aoiz, V. J. Herrero, and V. Sáez, Chem. Phys. Lett. **161**, 270 (1989).
[36](a) D. C. Clary, Nature **344**, 588 (1990); (b) S. Borman, Chem. Eng. News **68**, 32 (1990).
[37]H. Buchenau, J. P. Toennies, J. Arnold, and J. Wolfrum, Ber. Bunsenges. Phys. Chem. **94**, 1231 (1990).
[38]J. Geddes, H. F. Krause, and W. L. Fite, J. Chem. Phys. **52**, 3296 (1970); **56**, 3298 (1972); **59**, 566E (1973).
[39](a) G. H. Kwei, V. W. S. Lo, and E. A. Entemann, J. Chem. Phys. **59**, 3421 (1973); (b) G. H. Kwei and V. W. S. Lo, *ibid.* **72**, 6265 (1980).
[40]D. P. Gerrity and J. J. Valentini, J. Chem. Phys. **81**, 1298 (1984).
[41]E. E. Marinero, C. T. Rettner, and R. N. Zare, J. Chem. Phys. **80**, 4142 (1984).
[42]R. Götting, H. R. Mayne, and J. P. Toennies, J. Chem. Phys. **80**, 2230 (1984); **85**, 6396 (1986).
[43]K. Tsukiyama, B. Katz, and R. Bershon, J. Chem. Phys. **84**, 1934 (1986).
[44]T. Dreier and J. Wolfrum, Int. J. Chem. Kinet. **18**, 919 (1986).
[45]R. Götting, J. P. Toennies, and M. Vodegel, Int. J. Chem. Kinet. **18**, 949 (1986).
[46](a) R. Götting, V. Herrero, J. P. Toennies, and M. Vodegel, Chem. Phys. Lett. **137**, 524 (1987); (b) H. Buchenau, V. J. Herrero, J. P. Toennies, and M. Vodegel, MOLEC VII: Abstracts of Invited Talks and Contributed Papers, Assissi, Perugia, 1988, p. 109.
[47]B. A. Collings, J. C. Polanyi, M. A. Smith, A. Stolow, and A. W. Tarr, Phys. Rev. Lett. **59**, 2551 (1987); **63**, 2160E (1989).
[48]S. A. Buntin, C. F. Giese, and W. R. Gentry, J. Chem. Phys. **87**, 1443 (1987).
[49]D. L. Phillips, H. B. Levene, and J. J. Valentini, J. Chem. Phys. **90**, 1600 (1989).
[50]J. C. Nieh and J. J. Valentini, Phys. Rev. Lett. **60**, 519 (1988).
[51]J. J. Valentini and D. L. Phillips, in *Advances in Gas Phase Photochemistry and Kinetics*, edited by N. M. R. Ashfold and J. E. Baggot (Royal Society of Chemistry, London, 1989), Vol. 2 and references cited therein.
[52]K. D. Rinnen, D. A. V. Kliner, and R. N. Zare, J. Chem. Phys. **91**, 7514 (1989) and references cited therein.
[53]D. A. V. Kliner, K. D. Rinnen, and R. N. Zare, Chem. Phys. Lett. **166**, 107 (1990).
[54]D. A. V. Kliner and R. N. Zare, J. Chem. Phys. **93**, 2107 (1990).
[55]S. A. Buntin, C. F. Giese, and W. R. Gentry, Chem. Phys. Lett. **168**, 513 (1990).
[56]R. E. Continetti, B. A. Balko, and Y. T. Lee, J. Chem. Phys. **93**, 5719 (1990).
[57]G. C. Schatz and A. J. Kuppermann, J. Chem. Phys. **65**, 4668 (1976).
[58]J. Z. H. Zhang and W. H. Miller, Chem. Phys. Lett. **153**, 465 (1988).
[59]J. Z. H. Zhang and W. H. Miller, J. Chem. Phys. **91**, 1528 (1989).
[60]D. E. Manolopoulos and R. E. Wyatt, Chem. Phys. Lett. **159**, 123 (1989).
[61]R. T. Pack and G. A. Parker, J. Chem. Phys. **90**, 3511 (1989).
[62]T. J. Park and J. C. Light, J. Chem. Phys. **91**, 974 (1989).
[63]K. Haug, D. W. Schwenke, Y. Shima, D. G. Truhlar, J. Zhang, and D. J. Kouri, J. Phys. Chem. **90**, 6757 (1986).
[64]M. Mladenovic, M. Zhao, D. G. Truhlar, D. W. Schwenke, Y. Sun, and D. J. Kouri, Chem. Phys. Lett. **146**, 358 (1988).
[65]M. Mladenovic, M. Zhao, D. G. Truhlar, D. W. Schwenke, Y. Sun, and D. J. Kouri, J. Phys. Chem. **92**, 7035 (1988).
[66]M. Zhao, D. G. Truhlar, D. J. Kouri, Y. Sun, and D. W. Schwenke, Chem. Phys. Lett. **156**, 281 (1989).
[67]N. C. Blais, M. Zhao, M. Mladenovic, D. G. Truhlar, D. W. Schwenke, Y. Sun, and D. Kouri, J. Chem. Phys. **91**, 1038 (1989).
[68]N. C. Blais, M. Zhao, D. G. Truhlar, D. W. Schwenke, and D. J. Kouri, Chem. Phys. Lett. **166**, 11 (1990).
[69]M. Zhao, D. G. Truhlar, D. W. Schwenke, and D. J. Kouri, J. Phys. Chem. **94**, 7074 (1990).
[70]M. Zhao, D. G. Truhlar, N. C. Blais, D. W. Schwenke, and D. J. Kouri, J. Phys. Chem. **94**, 6696 (1990).
[71]J. D. Kress, Z. Bacic, G. A. Parker, and R. T. Pack, J. Phys. Chem. **94**, 8055 (1990).
[72]W. H. Miller, Annu. Rev. Phys. Chem. **41**, 245 (1990).
[73]R. E. Continetti, J. Z. H. Zhang, and W. H. Miller, J. Chem. Phys. **93**, 5356 (1990).
[74]W. H. Miller and J. Z. H. Zhang, J. Phys. Chem. **95**, 12 (1991).
[75]N. C. Blais and D. G. Truhlar, J. Chem. Phys. **88**, 5457 (1988).
[76](a) D. G. Truhlar and A. Kuppermann, J. Chem. Phys. **52**, 3841 (1970); (b) G. C. Schatz and A. Kuppermann, Phys. Rev. Lett. **35**, 1266 (1975).
[77]A. Kuppermann, in *Potential Energy Surfaces and Dynamical Calculations*, edited by D. G. Truhlar (Plenum, New York, 1981).
[78](a) R. D. Levine and S. F. Wu, Chem. Phys. Lett. **11**, 557 (1971); (b) J. G. Muga and R. D. Levine, *ibid.* **162**, 7 (1989).
[79](a) R. B. Walker, E. B. Stechel, and J. C. Light, J. Chem. Phys. **69**, 2922 (1978); (b) F. Webster and J. C. Light, *ibid.* **85**, 4744 (1986).
[80]D. G. Truhlar and J. T. Muckerman, in *Atom–Molecule Collision Theory*, edited by R. B. Bernstein (Plenum, New York, 1979).
[81]R. N. Porter and L. M. Raff, in *Modern Theoretical Chemistry*, edited by W. H. Miller (Plenum, New York, 1976), Vol. 2, part B.
[82]L. M. Raff and D. L. Thompson, in *Theory of Chemical Reaction Dynamics*, edited by M. Baer (CRC, Boca Raton, Florida, 1985), Vol. 3.
[83]D. G. Truhlar, B. P. Reid, D. E. Zurawski, and J. C. Gray, J. Phys. Chem. **85**, 786 (1981).
[84](a) A. Kosmas, E. A. Gislason, and A. D. Jorgensen, J. Chem. Phys. **75**, 2884 (1981); (b) F. E. Budenholzer, S. C. Hu, D. C. Jeng, and E. A. Gislason, *ibid.* **89**, 1958 (1988).
[85]W. P. Press, B. P. Flannery, S. A. Teulosky, and W. T. Vetterling, Numerical Recipes (Cambridge University, Cambridge, 1988).
[86](a) R. C. Tolman, *Statistical Mechanics with Applications to Physics and Chemistry* (Chemistry Catalog, New York, 1927); (b) A. A. Frost and R. G. Pearson, *Kinetics and Mechanism* (Wiley, New York, 1962).
[87](a) R. Grice, Mol. Phys. **19**, 501 (1970); (b) I. W. M. Smith, J. Chem. Ed. **59**, 9 (1982).
[88]R. D. Levine and R. B. Bernstein, Chem. Phys. Lett. **105**, 467 (1984).
[89]N. C. Blais and D. G. Truhlar, Chem. Phys. Lett. **102**, 120 (1983).
[90]I. Schechter, R. Kosloff, and R. D. Levine, Chem. Phys. Lett. **121**, 297 (1985).
[91]B. A. Blackwell, J. C. Polanyi, and J. J. Sloan, Chem. Phys. **24**, 25 (1977).
[92]K. G. Tan and K. J. Laidler, J. Chem. Phys. **67**, 5883 (1977).
[93]G. H. Kwei and D. R. Herschbach, J. Phys. Chem. **83**, 1550 (1979).

This article is copyrighted as indicated in the article. Reuse of AIP content is subject to the terms at: http://scitation.aip.org/termsconditions. Downloaded to IP: 130.209.6.50 On: Fri, 19 Dec 2014 14:02:13